ANALYSIS OF PAPR REDUCTION IN 5G COMMUNICATION

A Thesis submitted in partial fulfilment of the Requirements for the degree of

Master of Technology

In

Electronics and Communication Engineering

Specialization: Communication and Networks

By

RAHUL GOPAL

Roll No. – 213EC5240

Department of Electronics and Communication Engineering

National Institute of Technology Rourkela

Rourkela, Odisha, 769008

ANALYSIS OF PAPR REDUCTION IN 5G COMMUNICATION

A Thesis submitted in partial fulfilment of the Requirements for the degree of

Master of Technology

In

Electronics and Communication Engineering

Specialization: Communication and Networks

By

RAHUL GOPAL

Roll No. – 213EC5240

Under The Guidance of

Prof. S. K. PATRA

Department of Electronics and Communication Engineering

National Institute of Technology Rourkela

Rourkela, Odisha, 769008

May 2015

DEPARTMENT OF ELECTRONICS AND COMMUNICATION ENGINEERING

NATIONAL INSTITUTE OF TECHNOLOGY, ROURKELA

ROURKELA- 769008, ODISHA, INDIA

CERTIFICATE

This is to certify that the work in this thesis entitled "**ANALYSIS OF PAPR REDUCTION IN 5G COMMUNICATION"** by **RAHUL GOPAL** is a record of an original research work carried out by him during 2014-2015 under my supervision and guidance in partial fulfilment of the requirement for the award of the degree of Master of Technology in Electronics and Communication Engineering (Communication and Networks), National Institute of Technology, Rourkela. Neither this thesis nor any part of it, to the best of my knowledge, has been submitted for any degree or diploma elsewhere.

Place: NIT Rourkela

Date: 26th May 2015

Dr. Sarat Kumar Patra

Professor

Dept. of E.C.E
National Institute of Technology
Rourkela – 769008.

DEPARTMENT OF ELECTRONICS AND COMMUNICATION ENGINEERING

NATIONAL INSTITUTE OF TECHNOLOGY, ROURKELA

ROURKELA- 769008, ODISHA, INDIA

Declaration

I certify that

a) The work comprised in the thesis is original and is done by myself under the supervision of my supervisor.

b) The work has not been submitted to any other institute for any degree or diploma.

c) I have followed the guidelines provided by the Institute in writing the thesis.

d) Whenever I have used materials (data, theoretical analysis, and text) from other sources, I have given due credit to them in the text of the thesis and giving their details in the references.

e) Whenever I have quoted written materials from other sources, I have put them under quotation marks and given due credit to the sources by citing them and giving required details in the reference

Rahul Gopal

213EC5240

Acknowledgements

The work posed in this thesis is by far the most substantial attainment in my life and it would be unimaginable without people who affirmed me and believed in me. First and foremost I evince my profound reverence and deep regards to my guide Prof. S K. Patra for exemplary guidance, supervising and constant encouragement throughout the course of this thesis. A gentleman embodied, in true form and spirit, I consider it to my good fortune to have consociated with him.

I would like to evince a deep sense of gratitude to estimable Prof. K. K. Mahapatra, Head of the Department of Electronics and Communication Engineering for providing us with best facilities and his timely suggestions.

I would like to express my gratitude and respect to Prof. S.K. Behera, Prof. S. Deshmukh, Prof. S. K. Das, Prof. S. Hiremath, Prof. S. Maiti for their support, feedback and guidance throughout my M. Tech course duration. My special thanks to Ph.D. scholar Varun Kumar for his help, cooperation and encouragement. I would like to thank all my friends who made my journey at NIT Rourkela an indelible and gratifying experience.

Finally, my heartfelt gratitude towards my family for their tireless love and support throughout my life. They taught me the value of hard work by their own life example. They gave me tremendous support during my stay in NIT Rourkela.

Rahul Gopal

Abstract

The goal of this thesis is to analyze PAPR reduction performance in 5G communication. 5G communication technology is beyond 4G and LTE technology and expected to be employed around 2020. Research is going on for standardization of 5G technology. One of the key objective of 5G technology is to achieve high data rate (10Gbps). For this a large bandwidth is needed. Since limited frequency resources are available, the frequency spectrum should be efficiently utilized to obtain high data rate. Also to utilize white space, cognitive radio networks are needed. In cognitive radio network very low out of band radiation is desired. OFDM is used in 4G communication but it has the drawback of low spectral efficiency and high out of band radiation, which makes it a poor choice for 5G communication. So for 5G communication new waveform is required. FBMC, UFMC, GFDM are some of the waveform candidates for 5G communication. FBMC is a potential candidate for 5G communication and it is used in many 5G projects around the world. In this thesis FBMC is used as a waveform candidate for 5G communication. High PAPR is always a problem in multicarrier communication system. FBMC is also a multicarrier communication system, so it also suffers from high PAPR problem. To reduce the PAPR several PAPR reduction techniques have been proposed over the last few decades. Tone injection and companding are two promising techniques, which are used in PAPR reduction of multicarrier communication system.

In this thesis a combined scheme of tone injection and companding is used, which gives significant performance improvement compared to the tone injection and companding techniques taken separately. Simulation is performed to analyses the PAPR and BER performance of FBMC-FMT and FBMC-SMT system. Also a new clipping based PAPR reduction scheme is proposed in this thesis. For this scheme simulation is performed to analyze the PAPR performance of FBMC-FMT, FBMC-SMT and FBMC-CMT system. All the simulations are performed in MATLAB.

Contents

ABBREVIATION

ACE : Active Constellation Extension

ACP : Aggressive Clipping Projection

BER : Bit Error Rate

BFDM : Bi-orthogonal Frequency Division Multiplexing

BS : Base Station

CCDF : Cumulative Complementary Distribution Function

CMT : Cosine Modulated Multitone

CR : Cognitive Radio

DAS : Distributed Antenna System

DSL : Digital Subscriber Line

DWMT : Discrete Wavelet Multitone

FBMC : Filter Bank Multi Carrier

FMT : Filtered Multitone

GFDM : Generalized Frequency Division Multiplexing

ICI : Inter Carrier Interference

IOTA : Isotropic Orthogonal Transform Algorithm

ISI : Inter Symbol Interference

LTE : Long Term Evolution

MCM : Multi Carrier Modulation

MIMO : Multiple Input Multiple Output

OFDM : Orthogonal Frequency Division Multiplexing

OQAM : Offset Quadrature Amplitude Modulation

PAM : Pulse Amplitude Modulation

PAPR : Peak to Average Power Ratio

PHYDYAS : Physical layer for dynamic spectrum access and cognitive radio

PLC : Power Line Communication

PTS : Partial Transmit Sequence

QAM : Quadrature Amplitude Modulation

SER : Symbol Error Rate

SLM : Selected Mapping

SMT : Staggered Multitone

TI : Tone Injection

TR : Tone Resevation

UFMC : Universal Filter Multi Carrier

UWB : Ultra Wide Band

VLC : Visible Light Communication

VSB : Vestigial Side Band

WFDS : Weighted Frequency De-Spreading

WFS : Weighted Frequency Spreading

5G : Fifth Generation

NOMENCLATURE

D : Extension size

A : Clipping level

d : Distance between constellation points

N : Number of sub-channels

M : Filter length

c_{clip} : Clipped off portion of the signal

C_k : Extension vector

C_{clip} : Frequency domain representation of clipped signal

s_{clip} : Clipped signal for tone injection

E_i : Largest magnitude sample

k_1 : Maximum peak reduction sub-carrier

n_1 : Peak point

μ : Companding factor for μ -law

T : Symbol duration

s_k : Signal of k^{th} sub-carrier

$d_{k,n}$: Symbol with k^{th} sub-carrier and n^{th} symbol

K : Overlapping factor

H_k : prototype filter coefficient

S/P : Serial to parallel

P/S : Parallel to serial

A/D : Analog to Digital

D/A : Digital to analog

η_{max} : Maximum efficiency of power amplifier

f_k : Snthesis filter with k^{th} sub-carrier

h_k : Analysis filter with k^{th} sub-carrier

h_p : Prototype filter

LIST OF FIGURES

LIST OF TABLES

Chapter 1

INTRODUCTION TO 5G TECHNOLOGY

1

INTRODUCTION TO 5G TECHNOLOGY

Currently, fourth generation wireless communication systems have been employed in most of the countries in the world. However, there are still some challenges like an explosion of wireless mobile devices and services, which cannot be accommodated even by 4G, such as the spectrum scarcity and high energy consumption [1]. Wireless system designers are continuously facing the increasing demand for mobility required and high data rates by new applications and that's why they have started research on fifth generation wireless systems that are expected to be employed beyond 2020. 5G technology stands for fifth generation mobile technology which is the standard beyond 4G and LTE-advanced.

There are different challenges in 5G, to overcome these we need new breakthroughs and new technologies. Some of the promising technologies for 5G communication are massive MIMO, cognitive radio, visible light communications, spatial modulation, mobile femtocell, green communication. Also we need new cellular architecture for 5G.

5G challenges:

- To serve extremely large amount of users
- Efficiently use of spectrum
- Reduce power consumption
- To support high mobility
- To support avalanche of traffic volume 1000× in ten years
- To support large diversity of user cases and requirement

Technical objectives:

- 1000 × data volume
- 10-100 × higher number of connected devices
- Up to 10 Gbps end user data rate
- 5 × lower latency
- 10 × longer battery life

Features:

- Massive MIMO
- Ultra dense networks
- Moving networks
- Higher frequencies
- Device to device communication
- Ultra reliable communication
- Massive machine communication
- Fiber like user experience
- Ultra-fast switching

Necessary breakthroughs:

- For high spectral efficiency, advance waveform technologies, coding and modulation algorithm are essential
- New architectures are required to enable computationally intensive and adaptive new air interface
- An advance in RF domain processing will required to bring benefits of the efficient and flexible use of spectrum. Single frequency full duplex radio technology will be major contribution to spectrum efficiency
- In radio technology to support vast range of capabilities from ultra-low energy to ultra-fast device with long lasting battery life
- Virtualization and cloud based radio access infrastructure
- Mass scale MIMO
- 5G devices

1.1 A potential 5G wireless cellular architecture

To address the above challenges and meet 5G system requirements we require a dramatic change in the design of cellular architecture [1]. One of the key ideas to design the 5G cellular architecture is to separate outdoor and indoor scenario. Because 80% of the time we are in indoor condition, and there is a huge penetration loss through building. So we need to avoid this situation. This will be associated with distributed antenna system (DAS) and massive MIMO.

In this architecture outdoor base stations (BSs) will be equipped with large antenna arrays with some antenna elements distributed around the cell and connected to the BSs via optical fibers benefiting from both DAS and massive MIMO technologies. Outdoor mobile users are generally with limited numbers of antenna elements but they can collaborate with each other to form a virtual massive MIMO links. Outside of every building large antenna arrays will also be installed to communicate with outdoor BSs or DA elements of BSs possibly with LOS component. Using this type of cellular architecture as indoor users only required to communicate with indoor access points with large antenna arrays installed outside of the buildings. Many technologies can be used for short-range communication with high data rates. Some examples are femtocell, Wi-Fi, ultra wide band (UWB), mm-wave communication, visible light communication (VLC).

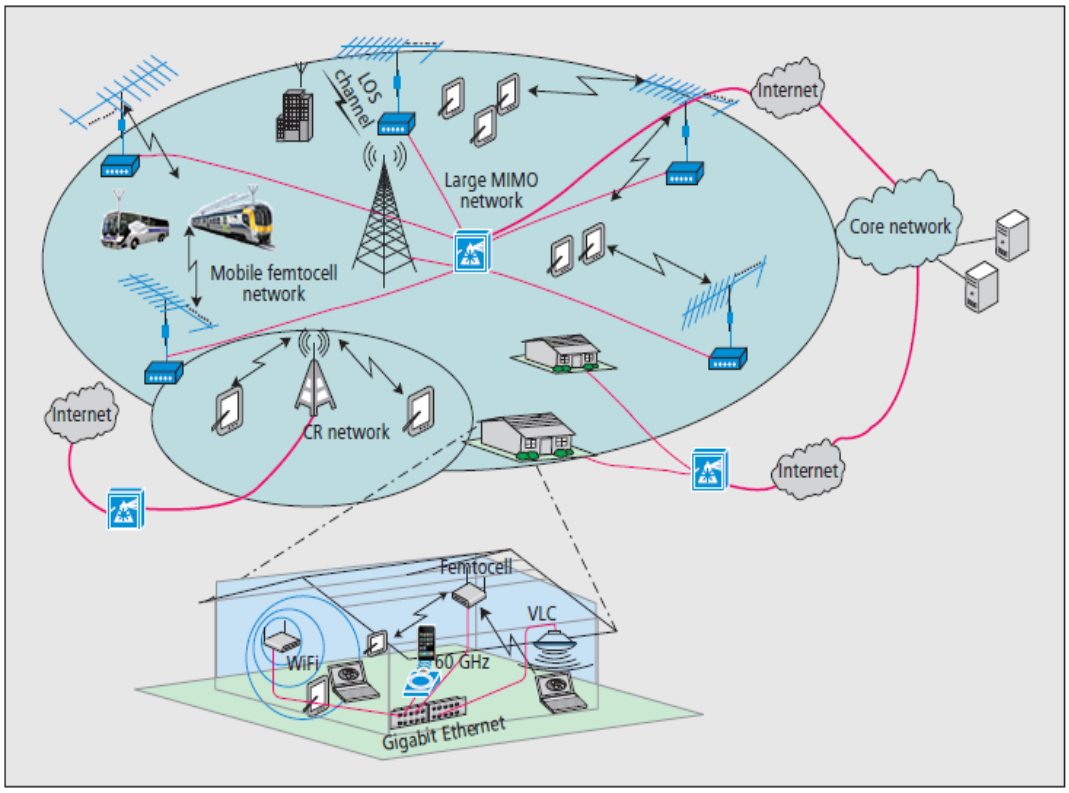

Fig. 1.1 A potential 5G wireless cellular architecture [1]

Besides finding unused spectrum, we can try to improve the utilization of existing frequency spectrum for example via cognitive radio networks. To accommodate high mobility users in a vehicle and in high-speed trains should use mobile femtocell concept. Mobile femtocells are located inside the vehicles to communicate with users within the mobile femtocell while large antenna arrays are located outside of a vehicle to communicate with outdoor BSs. A mobile femtocell and its associated users are all viewed as a single unit to the BS. From the user point of view, a mobile femtocell is seen as a regular BS.

1.2 Promising Key 5G Wireless Technologies

Massive MIMO:-In massive MIMO systems, the transmitter and receiver sections are equipped with a large number of antenna elements (generally ten or even hundreds). These antenna elements can be co-located or distributed. Besides conventional MIMO system, massive MIMO can also significantly enhance spectral and energy efficiency of the system. Also the effect of noise and fast fading vanishes.

Cognitive radio networks:-Cognitive radio is an innovative software defined radio technology which is used to improve the utilization of the congested RF spectrum. CR is motivated by the fact that a large portion of the radio spectrum is underutilized most of the

time. In CR systems, a secondary system can share spectrum either on an interference-free basis or an interference tolerance basis.

Mobile femtocell:-It combines the mobile relay concept (moving network) with mobile femtocell technology. A mobile femtocell is a small cell that can move around and dynamically change its connection to an operator's core network. It can be deployed in public bus, train or in private cars to enhance quality of service to users within vehicles. Spectral efficiency of the entire network is also improved by the mobile femtocell. It contributes to signaling overhead reduction of the network.

Visible light communication:-VLC uses white light LEDs for signal transmission and PIN photodiodes or avalanche photodiodes as signal receivers. If illumination is not required, then infrared LEDs can also be used. In VLC, information is carried by intensity (power) of the light. Data rate of 3.5 Gbps is reported from a single LED.

Green communication:-The design of 5G system should minimize energy consumption in order to achieve greener wireless communication system. The macro cell BS will have less pressure in allocating radio resources if indoor and outdoor traffic are separated and can transmit with low power resulting in significant reduction in energy consumption. VLC and mm wave technologies are also considered as energy efficient wireless communication solution for 5G.

Future challenges in 5G wireless communication networks

- Optimizing performance matrices
- Reducing signal processing complexity for massive MIMO
- Realistic channel models for 5G wireless systems
- Interference management for CR network

1.3 Waveform contenders for 5G communication

OFDM is not suitable for 5G because of its low spectral efficiency and synchronization problem. So we have to search for new waveform contenders for 5G communication. Some of the promising waveform contenders are Generalized Frequency Division Multiplexing (GFDM), Universal Filtered Multicarrier (UFMC), Filter Band Multicarrier (FBMC) and Biorthogonal Frequency Division Multiplexing (BFDM).

GFDM:-Generalized frequency division multiplexing (GFDM) is a non-orthogonal, multicarrier communication scheme which is proposed to address emerging requirements in cellular communications system such as efficient use of spectrum and machine-to-machine

communication with special attention to asynchronous low duty cycle transmission and exploration of non-continuous bandwidths. In GFDM we can transmit multiple symbols per sub-carrier which is not possible in OFDM. GFDM uses block based transmission which is enabled by circular pulse shaping of the individual sub-carriers.

Out of band radiation is reduced by applying different length pulse shaping filters and cyclic prefix is used to reduce ISI and ICI.GFDM is a good choice for short burst application. As a generalization of OFDM, GFDM is compliant with OFDM when the number of symbols per subcarrier is chosen to be one. GFDM can reach BER performance of OFDM while out of band radiation can be reduced by using pulse shaped subcarriers and thus minimizing interference to the legacy system when it is used in cognitive radio application.

UFMC: - filter bank multicarrier (FBMC) filters the signal on per subcarrier basis while orthogonal frequency division multiplexing (OFDM) filters the signal on single shot. UFMC is a way between these two techniques. In UFMC we apply filtering to subsets of the complete band instead of single subcarriers or the complete band. In this way we can get the benefit of better subcarrier separation from FBMC and less complexity from OFDM. UFMC outperforms FBMC and OFDM in some, but not all, of the different aspects relevant for communication.

FBMC: - Filter Bank Multicarrier system consist of a bank of filters in transmitter and receiver side. These filters are frequency and phase shifted version of a prototype filter. Prototype filter is the basis of FBMC system which separate two symbols in such a way that minimum out of band radiation occurs. Prototype filter is designed to get low out of band radiation between subcarriers. In filter bank multicarrier (FBMC), the CP can be removed and subcarriers can be better localized in time and frequency, by using advanced prototype filter design. This makes it leading contender for 5G communication.

BFDM:-In bi-orthogonal frequency division multiplexing (BFDM) symbols can be perfectly recovered by using bi-orthogonality approach. bi-orthogonality is a weaker form of orthogonality,here transmit and receive pulses are no longer orthogonal to each other. This approach is well suited for transmission of long symbol pulses. It has the drawback that spectral regrowth is possible due to periodic setting when calculating the bi-orthogonal pulses

1.4 Objective

Objective of this thesis is to first choose a suitable waveform candidate for 5G communication. One of the key objective of 5G communication is to achieve high spectral efficiency and low out of band radiation. So we have to choose a waveform which satisfies above two criteria.

OFDM is a poor choice for 5G communication because it uses cyclic prefix which reduces the spectral efficiency of the system. Also high out of band radiation is a problem with OFDM. High PAPR has always been a problem with multicarrier systems which reduces the efficiency of power amplifier in the system. Power amplifier efficiency is directly related to PAPR. So power amplifier efficiency can be improved by reducing the PAPR of the signal, which will save power and cost of the system. Main objective of this thesis can be summarized as follows:

- Study and analyze different PAPR reduction techniques which can be applied in 5G communication.
- Modify existing PAPR reduction techniques to improve PAPR performance of the system.
- Designing receiver section to evaluate SER performance of the system.

1.5 Thesis organization

This thesis is organized into six chapters. The current chapter gives introduction of 5G technology. Objective of the thesis has been discussed and last section describes the complete thesis organization.

Chapter 2

In second chapter, Filter bank multicarrier system is introduced and described. Also survey on prototype filter and comparison between OFDM and FBMC is discussed in this chapter.

Chapter 3

In this chapter, peak to average power ratio is described with the effects of high PAPR. Different PAPR reduction technique and analysis of PAPR using CCDF is also discussed.

Chapter 4

The fourth chapter discusses Tone Injection and Companding technique of PAPR eduction.

Chapter 5

In the fifth chapter PAPR performance is analyzed for combined scheme of tone injection and companding techniques and for new clipping based PAPR reduction technique. Simulation results are shown and discussed.

Chapter 6

The sixth chapter presents conclusion and future scopes of this work.

Chapter 2

FILTER BANK MULTI CARRIER

2

FILTER BANK MULTI CARRIER

Filter bank multi carrier is a technique in which a bank of filters are used in transmitter and receiver side. Transmitter filter is called synthesis filter bank and receiver filter is called analysis filter bank. Interestingly, FBMC is the multicarrier technique, which was developed prior to OFDM.Chang is the first person who came with the idea of FBMC in the 1960s and also presented the conditions required for signaling a parallel set of pulse amplitude modulated(PAM)symbols going through a bank of overlapping vestigial side-band (VSB) modulated filters. A year later,[3] Saltzberg extended the idea of chang and showed how the method could be modified for transmission of quadrature amplitude modulated (QAM) symbols. Saltzberg showed that we can achieve the maximum spectral efficiency in FBMC system if a half-symbol space delay between the in-phase and the quadrature phase components of QAM symbols is maintained. In 1980s, Hirosaki works on FBMC and proposed an efficient polyphase implementation for the Saltzberg method. The method which is proposed by Saltzberg is called OFDM based on offset QAM or OFDM-OQAM. The offset comes from the fact that there is half symbol delay between the in-phase and quadrature component of each QAM symbol with respect to each other. This method is called staggered modulated multitone (SMT), where the word staggered comes from the fact that the in-phase and quadrature phase components in each QAM symbols are time staggered. In the 1990s the use of cosine modulated filter banks for data transmission was widely studied. The improvement in digital subscriber line (DSL) technology led to more work on two classes of FBMC communication systems, namely, filtered multitone (FMT) and discrete wavelet multitone (DWMT) modulation. It has been shown that DWMT is using cosine-modulated filterbanks .Therefore, DWMT was renamed to cosine-modulated multitone (CMT). CMT uses vestigial sideband (VSB) modulation to transmit PAM symbols. FMT is another FBMC method which is proposed for DSL applications. In FMT, no overlapping occurs between adjacent subcarriers. Therefore FMT is not bandwidth efficient compared to SMT and CMT.

Wireless channels are characterized by multipath fading. Which result in inter-symbol interference (ISI) in wireless channels. ISI in a channel is proportional to delay spread and also inversely proportional to symbol duration. Therefore by increasing the symbol period we can decrease ISI but it also decrease the data rate. In an MCM systems, a data stream is multiplexed into N parallel substreams, each of which has a N times slower rate. Therefore, the effect of ISI is reduced by factor N. The parallel data streams are modulated at N subcarriers and added together at the transmitter. At the receiver side N streams of symbols are separate band demultiplexes them to the original higher rate stream of symbols.

In multicarrier communication system OFDM is mostly used. OFDM is alternative technique for OFDM. In OFDM cyclic prefix is used to combat channel distortion. This channel distortion problem is solved in FBMC by using filtering technique. If we choose proper filter then interference is only between adjacent channels and there is no interference between non-adjacent channels. Thus FBMC technique is more suited for high mobility applications and here orthogonality may be destroyed which will not produce ICI unlike OFDM. Also big side lobes in OFDM is a problem which makes it difficult in cognitive radio application. To suppress the side lobes there would be up to 50% loss in bandwidth. So FBMC is a suitable candidate for 5G communication.

There are two class of FBMC. First class is used for transmission of real valued signal by using pulse amplitude modulation (PAM) and second class is used for transmission of complex valued signal by using quadrature amplitude modulation (QAM).

There are three methods to generate FBMC signal. These are FMT, CMT and SMT.

2.1 Staggered modulated multitone (SMT)

Staggered modulated multitone is an FBMC generation method which uses offset quadrature amplitude modulation (OQAM). OQAM is a form of quadrature amplitude modulation (QAM). In which we choose a root-Nyquist filter with symmetric impulse response for pulse-shaping at the transmitter side and the same filter at the receiver side in a multichannel QAM system, and we introduce a half symbol delay between the in-phase and quadrature-phase components of QAM symbols. This makes it possible to get baud-rate spacing between adjacent subcarrier, and we can still recover the information symbols, which is free from inter symbol interference (ISI) and inter carrier interference (ICI). In this method, unlike OFDM no cyclic prefix is required for resolving ISI and ICI. So OQAM method is more bandwidth efficient than OFDM. In SMT method as shown in fig. 2.1 N parallel data streams are first given to N filters and then in phase and quadrature phase components are staggered in time by half symbol duration, T/2.

Output of these filters are then modulated with N subcarriers, whose frequencies are separated by 1/T space.

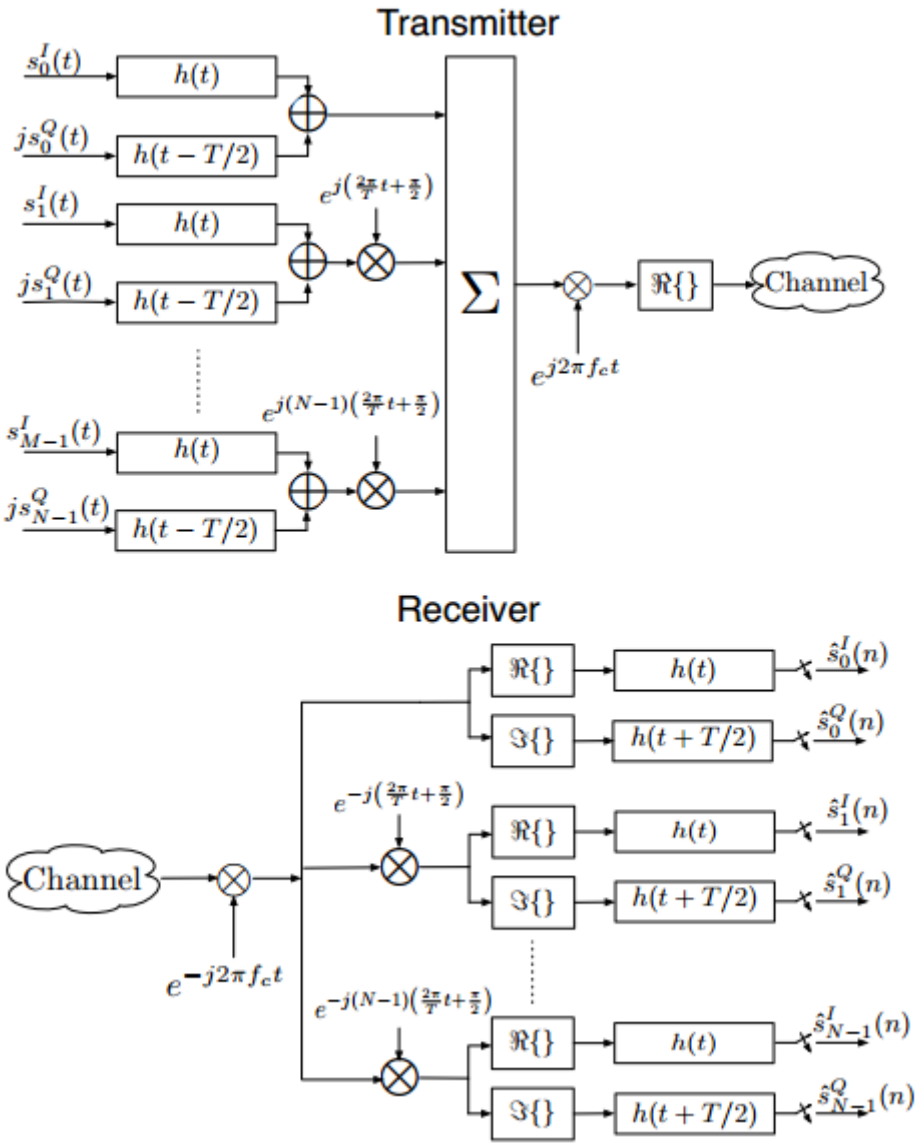

Fig. 2.1 Structure of SMT system

Suppose we have a complex symbol

$$x(t)=\sum_{m=0}^{N-1}\sum_{l=-\infty}^{\infty}s_m[l]h(t-nT)e^{j\frac{\pi}{2T}(t-lT)}e^{jm(\frac{2\pi t}{T}+\frac{\pi}{2})} \quad (1)$$

Where $s_k^I[n]$ is in phase component and $s_k^Q[n]$ is quadrature component of the k[th] subcarrier and n[th] symbol.Let us define $s_k^I(t)$ and $s_k^Q(t)$ as

$$s_k^I(t)=\sum_k s_k^I[n]\delta(t-nT) \quad (2)$$

$$s_k^Q(t)=\sum_k s_k^Q[n]\delta(t-nT) \quad (3)$$

Where $\delta(t)$ is the delta function. The complex-valued baseband SMT modulated FBMC signal is defined as

$$x(t)=\sum_{m=0}^{N-1}\sum_{l=-\infty}^{\infty}(s_m^I[l]h(t-nT)+js_m^Q[l]h(t-lT-T/2))e^{jm(\frac{2\pi t}{T}+\frac{\pi}{2})} \quad (4)$$

2.2 Cosine Modulated Multitone (CMT)

In CMT method, is used for transmission of real valued signal. It a set of vestigial side-band (VSB) sub carrier channels. Each carrier carry a stream of pulse amplitude modulated (PAM) symbols. This scheme also has the maximum bandwidth efficiency like SMT method. In CMT method *N* complex symbols can be transmitted on each multicarrier symbol, which require a system with 2*N* subcarrier where each carrier carry a real symbol, while, in an SMT system the transmitter would require *N* subcarriers which carry *N* complex symbols. If we transmit SMT symbols at the rate of 1/*T* complex symbols on each subcarrier with a bandwidth of 1/*T*, an equivalent CMT system with the same data rate, will have a data rate of 1/*T* real symbols on each subcarrier with the bandwidth of 1/2*T*. Therefore, to achieve the same data rate as SMT, bandwidth is divided into twice as many subcarriers in case of CMT.

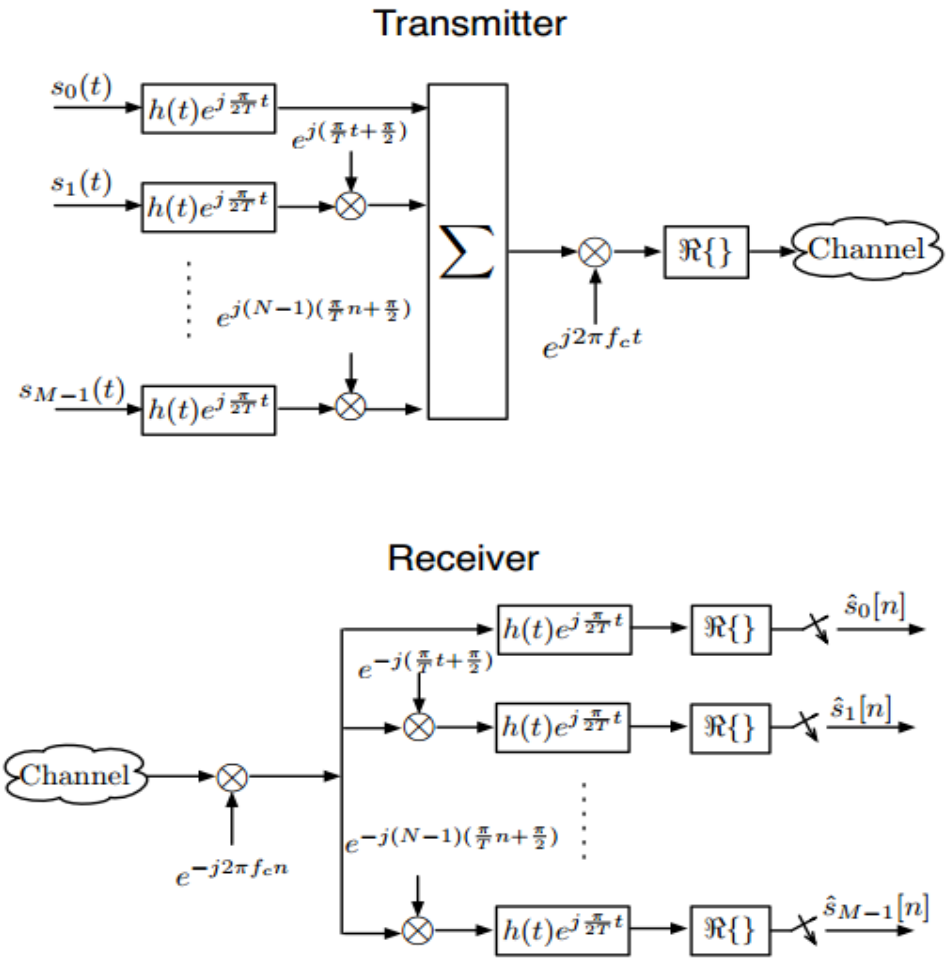

Fig. 2.2 structure of CMT system

In Fig. 2.2 the structure of a CMT MCM system is shown. Here input PAM symbols are band limited by a synthesis filter bank to get vestigial sideband signals and then modulate them to various frequency bands.To perform vestigial sideband filtering a frequency shifted version of a lowpass filter $h(t)$, centred at $f = \pi/2T$ with impulse response $h(t)e^{j\frac{\pi}{2T}t}$ is used. Transmitted symbols sequence in a CMT system can be presented as

$$s_m(t) = \sum_n s_m[n]\delta(t - nT) \tag{5}$$

Where $s_m[n]$ are PAM symbols. According to Fig. 2.3, the baseband FBMC- CMT signal at the transmitter, $x(t)$, is obtained as

$$x(t) = \sum_{m=0}^{N-1} \sum_{l=-\infty}^{\infty} s_m[l]h(t - nT)e^{j\frac{\pi}{2T}(t-lT)} e^{jm(\frac{2\pi t}{T}+\frac{\pi}{2})} \tag{6}$$

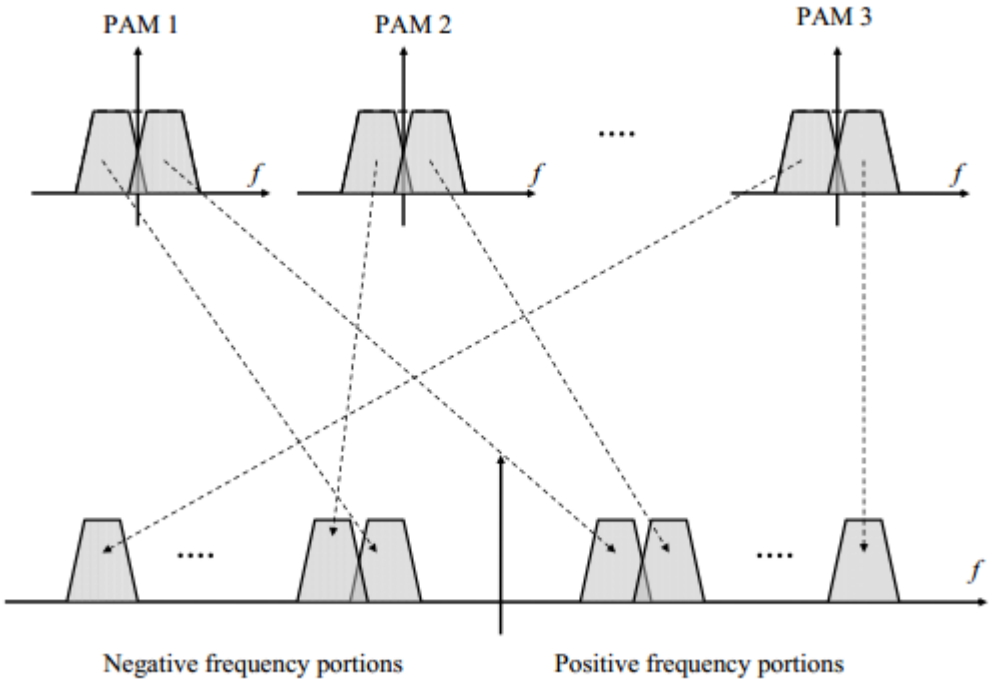

Fig. 2.3 CMT modulation

2.3 Filtered Multitone (FMT)

In FMT method, subcarriers are arranged in such a way that adjacent subcarriers do not overlap. As such, FMT may be seen as a MCM technique that follows the principle of frequency division multiplexing (FDM) .In FMT method, a high-rate data stream is separated into a number of disjoint frequency bands. However, in order to keep the subcarrier bands non-overlapping, guard bands are required, which needs excess bandwidth to allow for a transition

band for each subcarrier. Hence, this method is not a bandwidth efficient method due to the guard bands in FMT communication systems. FMT method is similar to a conventional frequency division multiplexing method. There is no ICI problem in this method because no overlap between adjacent subcarriers occur.

2.4 OQAM Pre-Processing

OQAM Pre-Processing and post processing blocks are required for generation of FBMC signal by SMT method [3]. Pre-processing block which transform signal from QAM to OQAM is shown in Fig. 2.4 [4]. Here first operation is complex to real conversion, where real and complex part of input symbol $c_{k,l}$ is separated into two new symbols $d_{k,2l}$ and $d_{k,2l+1}$. Sub-channel number determines the order of these new symbols, i.e. for even and odd number of sub-channels conversion is different. In complex to real conversion sample rate is increased by 2. After this symbols are multiplied by $\theta_{k,n}$ sequence.

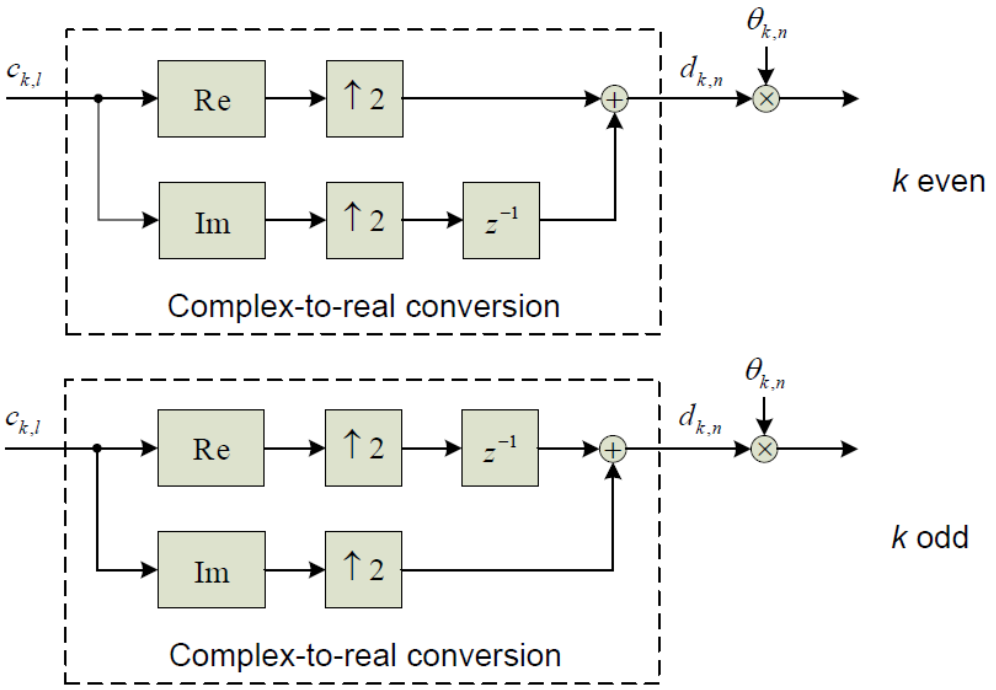

Fig. 2.4 OQAM Pre-Processing section

2.5 OQAM Post Processing

In Fig. 2.5 post processing block is shown and there are two structures for post processing as shown [4]. First input data is multiplied by $\theta^*_{k,n}$ sequence and then real part of this signal is taken. After that real to complex conversion is performed, where two successive complex valued symbols (with one multiplied by j) gives a real symbol $\hat{c}_{k,n}$. Here sample rate is

decreased by 2. In this way we can convert QAM signal to OQAM signal for generation of FBMC by SMT method and also convert back from OQAM to QAM signal.

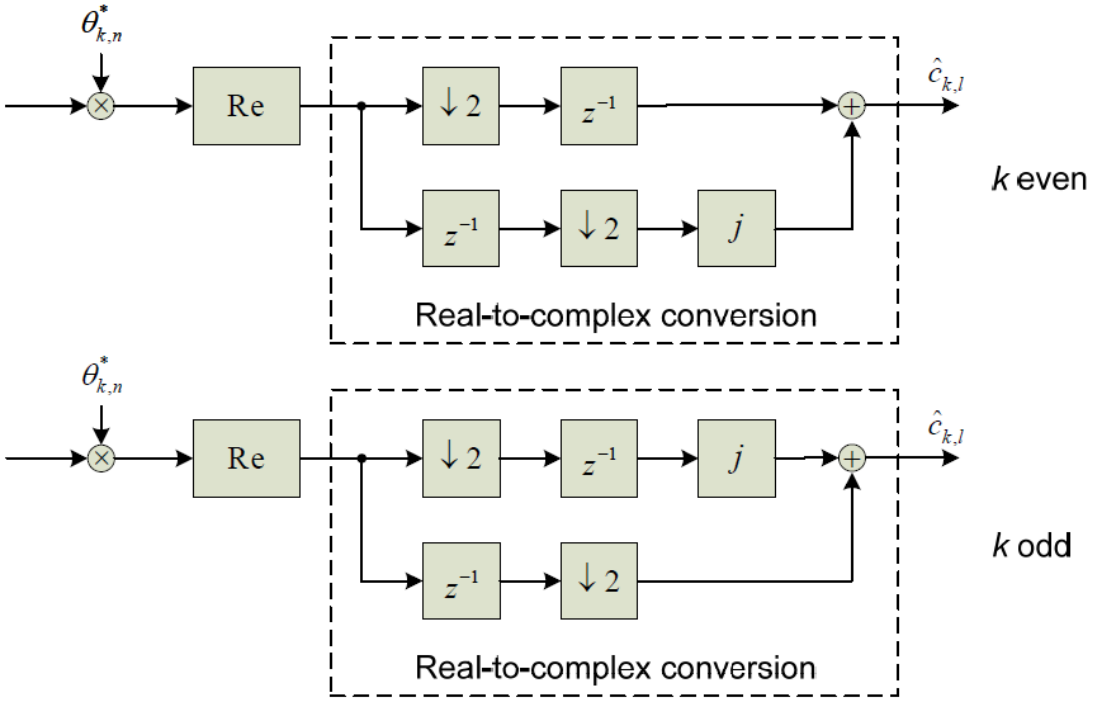

Fig. 2.5 OQAM post processing block

Time-frequency lattice and sub-channel spectrum is shown in Fig. 2.6 time frequency lattice represents orientation of OQAM symbols in time and frequency domain [5]. Symbol spacing is T/2 and sub-channel spacing is 1/T.

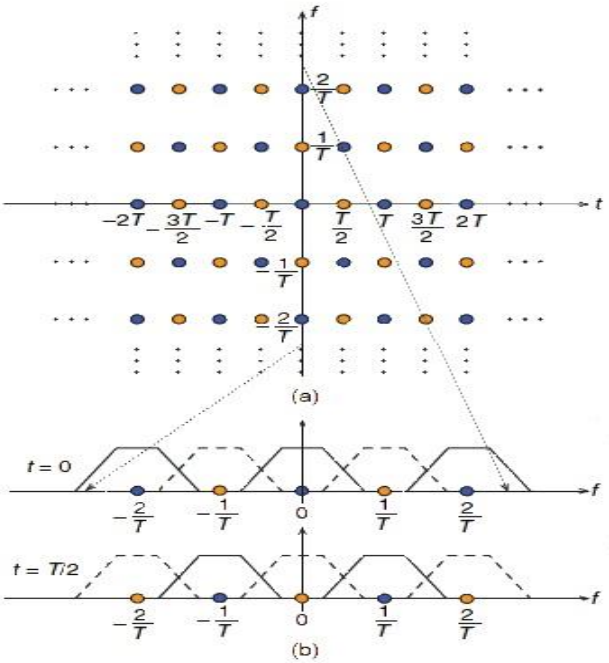

Fig 2.6 (a) Time-frequency lattice representation of FBMC-OQAM symbols

(b) Demonstration of the sub-channel spectra for t=0 and t=T/2

2.6 PHYDYAS Prototype Filter Design

Physical layer for dynamic spectrum access and cognitive radio (PHYDYAS) is a project in 5G communication[4]. PHYDYAS prototype filter is originally designed by Bellanger, which is accepted as prototype filter for most of the FBMC projects. In this filter nyquist criteria is satisfied by considering the frequency coefficients and imposing the symmetry condition.
In communication system, global nyquist filter is designed by splitting the filter in two parts, half nyquist filter in both transmitter and receiver side. To satisfy the symmetry condition, squares of the frequency coefficients are taken. The frequency coefficients of the half nyquist filter for overlapping factor K=2,3 and 4 are given by

Table 2.1 PHYDYAS prototype filter coefficients

K	H_0	H_1	H_2	H_3
2	1	0.707106	-	-
3	1	0.911438	0.411438	-
4	1	0.971960	0.707106	0.235147

The impulse response of the PHYDYAS filter is given as

$$h(t) = \begin{cases} \frac{1}{\sqrt{A}}[1+2\sum_{k=1}^{K-1}(-1)^k H_k cos(\frac{2\pi kt}{KT})] & t \in [0, KT] \\ 0 & elsewhere \end{cases} \quad (7)$$

Where A is normalization constant

$$A = KT\left[1+2\sum_{k=1}^{K-1} H_k^2\right] \quad (8)$$

Fig. 2.7 shows[3] the frequency response of prototype filter for K=4. In prototype filter the frequency response consist of 2K-1 pulses.
In this filter out-of-band ripples are reduced significantly and a highly selective filter has been obtained.

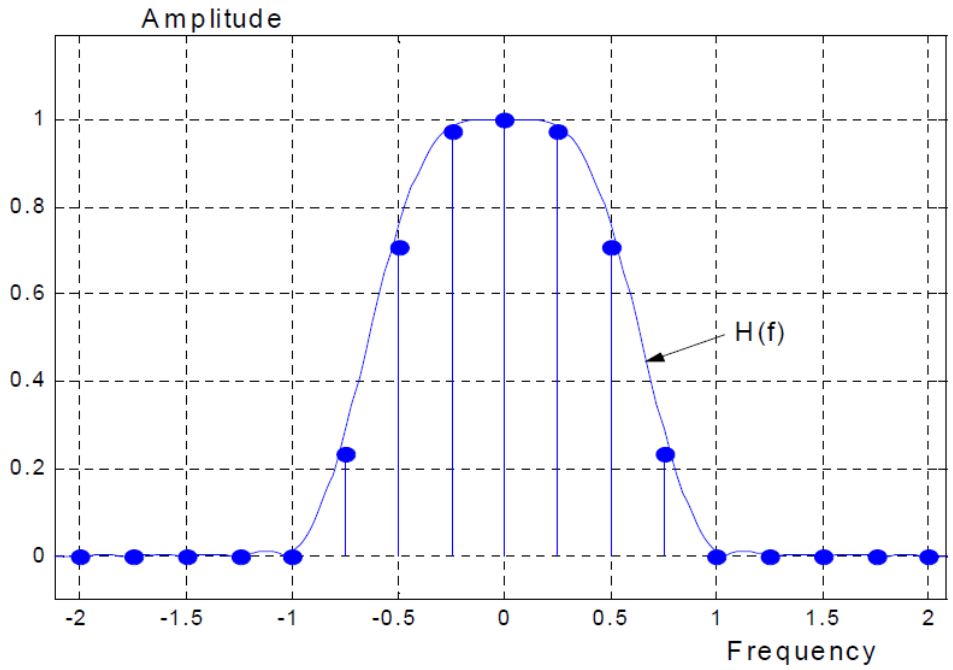

Fig. 2.7 Frequency response of prototype filter for K=4

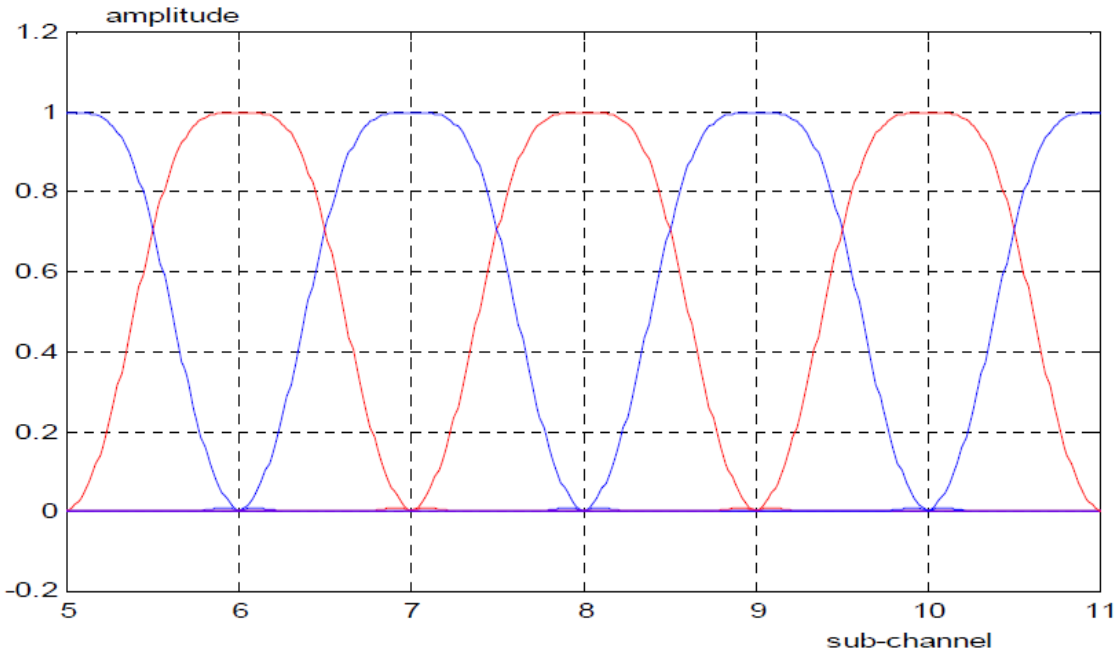

Fig. 2.8 Frequency response of a section of FBMC system

To obtain filter bank structure from prototype filter we have to perform the frequency shift operation for each sub-carrier.To getthe filter with index *k* we have to multiply the prototype filter coefficients by $e^{j2\pi ki/M}$ .Fig 2.8 shows[3] the frequency response of a section of FBMC system based on PHYDYAS prototype filter with K=4. Where the frequency spacing between

subcarriers is taken as unity. Here we can observe that odd index (even index) sub-carriers do not overlap to each other. They overlap with neighbors only. Which is the main characteristic of FBMC system.

2.7 FBMC system implementation with IFFT

FBMC system can be implemented by using IFFT and FFT blocks [3]. Which is shown [3]in Fig. 2.9. In OFDM system input data stream is modulated by one sub-carrier but in case of FBMC, with overlapping factor K, a data stream modulates 2K-1 sub-carriers. Which requires IFFT of size KM. here first a data element $d_i(mM)$ is multiplied with filter coefficients and then fed to 2K-1 IFFT inputs with (i-1)K+1,…..,(i+1)K-1 indices. This process of spreading data over different IFFT inputs is called "weighted frequency spreading"

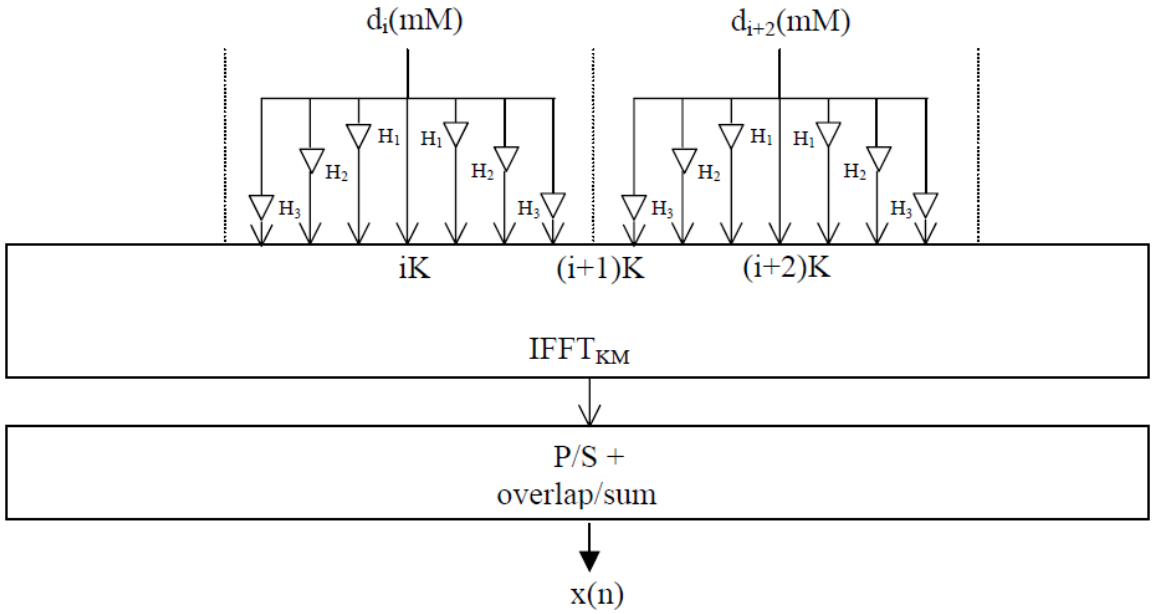

Fig. 2.9 weighted frequency spreading and IFFT

Fig. 2.9 shows the implementation of weighted frequency spreading for overlapping factor K=4. Here the sub-channels with indices i and i+2 are separated and do not overlap but sub-channels i+1 overlaps with i and i+2. To maintain orthogonality between adjacent sub-carriers i and i+2 are fed by real inputs and i+1 is fed by imaginary, or the inverse.

At the receiver side FFT of KM size is used. To recover the input data a weighted frequency despreading operation is performed on FFT output data. This operation is shown in Fig. 2.10 WFDS depends [3] on following property of Nyquist filter coefficients

$$\frac{1}{K}\sum_{k=-(K-1)}^{(K-1)}\left|H_k\right|^2=1 \qquad (9)$$

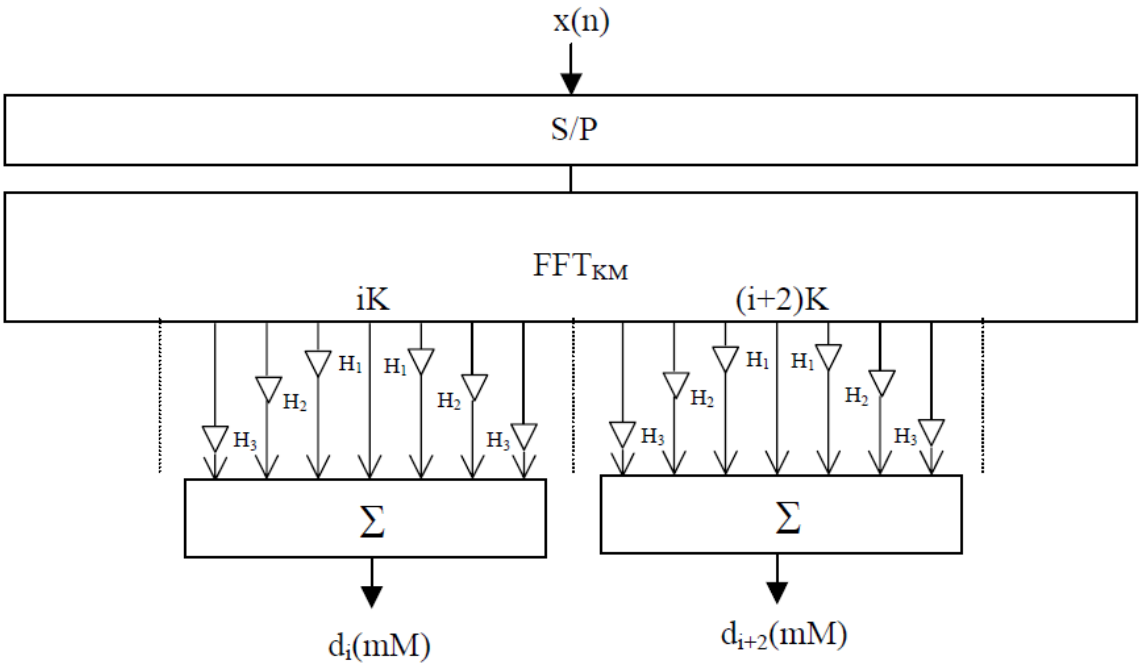

Fig. 2.10 weighted frequency despreading

2.8 A survey on prototype filter for FBMC

Filter bank multicarrier system is characterized by its prototype filter. Design of prototype filter is different for different purpose [6].There are number of filters which can be used in FBMC according to requirement. Filters are classified into three categories based on their theoretical definitions.

- Time limited filters
- Band limited filters
- Localized filters

Time limited filters:- Time-limited filters are those filters which are defined for finite durations as the name implies. As these filters are defined for finite durations the spectrum of these filters are infinite length. Since these filters are specifically design for finite duration, systems implementation is easy with these filters.

1. **Rectangular filter: -** Rectangular prototype filter is defined by a rectangular pulse in time domain and a sinc function in frequency domain. It is used in OFDM as prototype filter. Out of band radiation is is very high in this filter so cyclic prefix is required in OFDM system to overcome this problem.
2. **Window based filter:-** Windowing technique is used for designing prototype filter. There are numbers of windowing techniques with different side lobe characteristics.

Some of the popular windowing techniques are Hanning, Hamming, Blackman, Blackman-Harris. These technique are defined by their mathematical equation which are given as

3. **Optimal Finite Duration Pulse/Prolate Filter: -** In FBMC system truncation of filter is required to reduce the computational complexity with some undesired side lobes. So a tradeoff between side lobes and complexity is chosen to get a time limited pulse with minimum side lobes. Prolate filter is filter with these characteristics.
4. **Kaiser filter: -** This is an efficient filter which uses Bessel function to achieve the required characteristics. It offers an optimal solution for the out of- band radiation. A favorable property of Kaiser Filter is that by using a single design parameter β it can control the side lobes and stop-band attenuation.
5. **PHYDYAS filter: -** PHYDYAS prototype filter is originally designed by Bellanger, which is accepted as prototype filter for most of the FBMC projects. In this filter nyquist criteria is satisfied by considering the frequency coefficients and imposing the symmetry condition. This filter is characterized by its filter coefficients.

Band-limited Filters: - These filters are defined by finite bandwidth. However, they ideally require infinite time duration. Therefore these filters are problematic with practical consideration.

1. **Raised Cosine Filter: -** Raised-cosine filter is a Nyquist filter which is commonly used. In this filter the time-frequency localization is controlled by a parameter called as the roll-off factor α. This filter become rectangular filter when $\alpha=0$. Filter bandwidth is given by $(1+\alpha)/T$.
2. **Root Raised Cosine Filter: -** Root rised cosine filter is used in a transceiver to satisfy nyquist criteria. This filter is derived from rised cosine filter. If $P_{RC}(f)$ is the frequency response of rised cosine filter and $P_{RRC}(f)$ is the frequency response of root rised cosine filter, then these two are related by $P_{RC}(f) = P_{RRC}(f)\, P_{RRC}(f)$.
3. **Half Cosine and Half Sinc Filters: -** Half cosine filter is the RRC filter with $\alpha=1$. This filter gives good time/frequency behavior. It is characterized by small transition band with high attenuation in stop band.

Localized Filters: - In time-limited and band-limited filters area localized in only one domain but localized filters consider both domain on an equal footing. So they these filters provide compactness in both time and frequency domains. These filters are like Gaussian pulse.

1. **Gaussian filter: -** Its time and frequency behavior is same. Frequency response of a Gaussian function is also another Gaussian function. α_g is the control parameter in Gaussian filter. For α_g =1 gaussian filter is perfectly isotropic.
2. **Hermite pulse:-** This filter is commonly used in literature to obtain localized pulse shapes in doubly dispersive channels. Tis filter is obtained from Hermite polynomial function $H_n(t)$ with different order n.
3. **Isotropic Orthogonal Transform Algorithm (IOTA) filter**: - The isotropic orthogonal transform algorithm (IOTA) filter keep the excellent localization property of Gaussian filter, and provide orthogonality to prevent ISI and ICI between neighboring symbols in time/frequency lattice. With these parameters, IOTA filter works as a optimal Nyquist filter in terms of time-frequency localization when we consider rectangular lattice.

Table 2.2 Comparison of Filters

Filter	Analytical Model	Comments
Rectangular	$p(t) = \begin{cases} 1\ , & \lvert t\rvert \le \frac{1}{2} \\ 0\ , & \text{otherwise} \end{cases}$	It distributes the symbol energy uniformly in time domain. It is the prototype filter for CP-OFDM scheme.
Hanning (Raised-cosine)	$p(t) = \begin{cases} \frac{1}{2} + \frac{1}{2}\cos(2\pi t)\ , & \lvert t\rvert \le \frac{1}{2} \\ 0\ , & \text{otherwise} \end{cases}$	The function itself and its first derivative are continuous. Hence, the power of the sidelobes fall at $1/\lvert\omega\rvert^3$ per octave.
Exact Hamming	$p(t) = \begin{cases} \frac{25}{46} + \frac{21}{46}\cos(2\pi t)\ , & \lvert t\rvert \le \frac{1}{2} \\ 0\ , & \text{otherwise} \end{cases}$	Exact Hamming filter places zero at the position of the first sidelobe.
Exact Blackman	$p(t) = \begin{cases} \frac{7938}{18608} + \frac{9240}{18608}\cos(2\pi t) + \frac{1430}{18608}\cos(4\pi t)\ , & \lvert t\rvert \le \frac{1}{2} \\ 0\ , & \text{otherwise} \end{cases}$	Exact Blackman filter places zeros at the positions of the the third and fourth sidelobes.
Tapered-cosine-in-time (Tukey)	$p(t) = \begin{cases} 1\ , & \lvert t\rvert \le \frac{1-\alpha}{2} \\ \frac{1}{2} + \frac{1}{2}\cos\left(\frac{\pi}{\alpha}\left(\lvert t\rvert - \frac{1-\alpha}{2}\right)\right)\ , & \frac{1-\alpha}{2} < \lvert t\rvert \le \frac{1+\alpha}{2} \\ 0\ , & \text{otherwise} \end{cases}$	It is the rectangular filter where the edges are tapered by convolving a rectangular function with a cosine lobe. When $\alpha = 1$, it corresponds to Hanning filter.
Tapered-cosine-in-frequency (Tukey)	$p(t) = \frac{\sin(\pi t)}{\pi t}\frac{\cos(\pi\alpha t)}{1-4\alpha^2 t^2}$	It distributes the symbol energy uniformly in frequency domain when $\alpha = 0$.
Root-raised-cosine	$p(t) = \begin{cases} 1 - \alpha + 4\frac{\alpha}{\pi}, & t = 0 \\ \frac{\alpha}{\sqrt{2}}\left[\left(1+\frac{2}{\pi}\right)\sin\left(\frac{\pi}{4\alpha}\right) + \left(1-\frac{2}{\pi}\right)\cos\left(\frac{\pi}{4\alpha}\right)\right], & t = \pm\frac{1}{4\alpha} \\ \frac{\sin\left((1-\alpha)\pi t\right) + 4\alpha t\cos\left((1+\alpha)\pi t\right)}{\pi t\left(1-16\alpha^2 t^2\right)}\ , & \text{otherwise} \end{cases}$	It corresponds to tapered-cosine-in-frequency after matched filtering.
Mirabbasi-Martin	$p(t) = \begin{cases} a_0 + 2\sum_{l=1}^{K-1} a_l\cos(2\pi l t)\ , & \lvert t\rvert \le \frac{1}{2}\ , \\ 0\ , & \text{otherwise} \end{cases}$ $k_l = (-1)^l a_l\ ,\ k_0 = -1\ ,\ k_l^2 + k_{K-l}^2 = 1\ ,\ k_0 + 2\sum_{l=1}^{K-1} k_l = 0\ ,$ $\sum_{l=1}^{K-1} l^q k_l = 0\ ,\ q \ge 2\ ,\ q \in \{2n \mid n \in \mathbb{Z}\}$	It provides rapid-decaying. Power of the sidelobes fall at $1/\lvert\omega\rvert^{(q+3)}$ per octave, where q is the derivation order. Last equation is utilized to construct a complete set of equations.
Prolate	$p(t) = \arg\min_{p(t)}\left\{\int_{-\infty}^{\infty}\lvert P(f)\rvert^2 df - \int_{-\sigma}^{\sigma}\lvert P(f)\rvert^2 df\right\}\ .$	It is the optimally-concentrated pulse in frequency for a given filter length and bandwidth.
Optimal finite duration pulses	$p(t) = \sum_{l=0}^{N} a_{2l}\psi_{2l,\tau,\sigma}(t)$	It is the optimally-concentrated pulse for a given duration and bandwidth, which also satisfies Nyquist criterion in both time and frequency.
Kaiser	$p(t) = \begin{cases} \frac{I_0\left(\beta\sqrt{1-4t^2}\right)}{I_0(\beta)}\ , & \lvert t\rvert \le \frac{1}{2} \\ 0\ , & \text{otherwise} \end{cases}$ $I_0(x) = 1 + \sum_{k=1}^{\infty}\left[\frac{(x/2)^k}{k!}\right]^2$	Kaiser filter has very similar time-frequency characteristics of prolate filter. Although it is suboptimum solution for concentration problem, its formulation is given in closed-from.
Modified Kaiser	$p(t) = \begin{cases} \frac{I_0\left(\beta\sqrt{1-4t^2}\right)-1}{I_0(\beta)-1}\ , & \lvert t\rvert \le \frac{1}{2} \\ 0\ , & \text{otherwise} \end{cases}$	In order to provide faster decaying, Kaiser window is modified to obtain zeros at $\lvert t\rvert = 1/2$.
Gaussian	$p(t) = (2\rho)^{1/4}e^{-\pi\rho t^2}\ ,\ P(f) = p_{\text{gaussian}}(t, 1/\rho)$	It is the optimally-concentrated filter when there are no restrictions on filter length and bandwidth and $\rho = 1$.
IOTA	$p(t) = \mathcal{F}^{-1}\mathcal{O}_{\tau_0}\mathcal{F}\mathcal{O}_{v_0}p_{\text{gaussian}}(t)$ $\mathcal{O}_a x(t) = \frac{x(t)}{\sqrt{a\sum_{k=-\infty}^{\infty}\lVert x(t-ka)\rVert^2}}\ ,\ x(t) \in \mathbb{R}$ $\mathcal{F}^{-1}X(f) = \int X(f)e^{-j2\pi ft}df\ ,\ \mathcal{F}x(t) = \int x(t)e^{j2\pi ft}dt$	IOTA yields optimally-concentrated function when there are no restrictions on filter length and bandwidth. It also fulfills Nyquist criterion after matched filtering.
Hermite	$p(t) = \sum_{l=0}^{N} a_{4l}\psi_{4l,\infty,\infty}(t)\ ,$ $\psi_{n,\infty,\infty}(t) = H_n\left(\sqrt{2\pi}t\right)e^{-\pi t^2}\ ,\ H_n(t) = (-1)^n e^{t^2}\frac{d^n}{dt^n}e^{-t^2}$	By deforming the Gaussian filter with the high-order Hermite functions, it obtains zero-crossings to satisfy Nyquist criterion. It has similar characteristics with IOTA.
Extended Gaussian	$p(t) = \frac{1}{2}\left[\sum_{k=0}^{\infty} d_{k,\rho,v_0}\left[p_{\text{gaussian}}(t + k/v_0, \rho) + p_{\text{gaussian}}(t - kv_0, \rho)\right]\right] \times$ $\sum_{l=0}^{\infty} d_{l,1/\rho,\tau_0}\cos(2\pi lt/\tau_0)$	It is a generalized family based on Gaussian function which gives the closed-form expression of the filter derived via IOTA.

Chapter 3

PEAK TO AVERAGE POWER RATIO

3

PEAK TO AVERAGE POWER RATIO

3.1 Introduction to PAPR

High PAPR is an important issue in FBMC system which reduces the efficiency of power amplifier used in the circuit. PAPR problem in any MCM system arises because of the fact that the output symbol of MCM system is the summation of symbols modulated on different subcarriers and there is a probability that all symbols have same phase which leads to a very high peak compared to the average value of the symbol. PAPR of an FBMC system is defined as the ratio of peak power to the average power[7].

In general, the PAPR of a complex envelope d[n] with length N can be written as

$$PAPR = \left(\frac{max\{|d[n]|^2\}}{E\{|d[n]|^2\}} \right) \tag{10}$$

Where $|d[n]|$ is amplitude of d[n] and E denote the expectation of the signal. PAPR in dB can be written as:

PAPR(dB) = 10log10(PAPR) (11)

3.2 Effect of High PAPR

The linear power amplifiers are used in the transmitter side of any communication system. For linear power amplifier the operating point should be in the linear region of operation. Because of the high PAPR the operating point moves to the saturation region hence[8], the clipping of signal peaks occurs which generates in-band and out-of-band distortion. So we should increase the dynamic range of the power amplifier to keep the operating point in the linear region which reduces efficiency and enhances the cost of the power amplifier. Hence, a trade-off exists between nonlinearity and efficiency. so we should reduce PAPR value to improve the efficiency of the power amplifier.

3.3 PAPR Reduction Techniques

There are so many techniques presents for the reduction of PAPR. Some of the important PAPR reduction techniques are illustrated below:

Clipping and Filtering

This is one of the simplest technique used for PAPR reduction. Clipping is a technique in which the amplitude of the input signal is limited to a predetermined value[9]. Let x[n] represent input signal and $x_c[n]$ denote the clipped version of x[n], which can be expressed as

$$x_c[n] = \begin{cases} -A & x[n] \leq -A \\ x[n] & |x[n]| < A \\ A & x[n] \geq A \end{cases} \quad (12)$$

Where A is the clipping level. However this technique has the following drawbacks:

- Clipping causes signal distortion, which results in degradation of Bit Error Rate performance.
- Out-of-band radiation also occurs in clipping, which is responsible for interference between adjacent channels. Filtering can be used to reduce this out-of-band radiation.
- Filtering of the clipped signal brings the peak regrowth. That means the signal level may exceed the clipping level after filtering operation because of the clipping operation. So we came to know that distortion occurs during the transmission of data in clipping and filtering technique.

Coding

In the coding technique, some code words are used to minimize or reduce the PAPR of the signal. It do not cause any distortion and also no out-of-band radiation produces, but it has a drawback of reduced bandwidth efficiency as the data rate is reduced. It also suffers from complexity issues [10], because it requires large memory for finding the best codes and to store large lookup tables, especially for a large number of subcarriers.

Partial Transmit Sequence

In the Partial Transmit Sequence (PTS) technique [11], an input data block of N symbols is partitioned into disjoint sub-blocks. A phase factor weights the sub-carriers in each sub-block for that sub-block. The phase factors are selected in such a way that the PAPR of the combined signal is reduced. But data rate loss occurs by using this technique.

Selected Mapping (SLM)

In the SLM technique, a number of alternative FBMC signals are generated from the input data block and one with minimum PAPR is chosen for transmission. Complexity and data rate loss are two drawbacks of this technique.

Tone Reservation

Tone reservation and tone injection are two efficient PAPR reduction techniques. In these techniques, a data block dependent time domain signal is appended to the original signal in such a way that peaks of the original signal will reduce. [14]This time domain signal can be easily computed at the transmitter side and can be easily removed at the receiver side.

In TR technique, some tones are reserved for transmission of peak reduction signals. So in this technique peak reduction signals are calculated and transmitted through reserved sub-carriers for PAPR reduction. Power increase and data rate loss are the drawbacks of this technique.

Tone Injection

The basic idea in TI technique is to increase the constellation size so that each of the points in the original basic constellation can be mapped into several equivalent points in the expanded constellation[15]. Here equivalent constellation points are added in original constellation point in a way that PAPR will reduce. These time domain signals for PAPR reduction is calculated for the sub-carrier which gives minimum PAPR. In this technique no data rate loss or distortion occurs but power increase in this technique.

Active Constellation Extension (ACE)

ACE technique is similar to Tone Injection technique. According to this technique [12], some of the outer signal constellation points in the data block are dynamically extended towards the outside of the original constellation such that PAPR of the data block is reduced. In this method also power increase of transmitted signal take place.

Companding

In Companding technique, we enlarge the small signals while compressing the large signals so that the immunity of small signals from noise will increase[13]. This compression is carried out at the transmitter end after the output is taken from IFFT block. There are two types of companders: μ-law and A-law companders. Compression of the signal reduces high peaks, so in this way PAPR reduction of input signal take place. This is a simple and low complexity method for PAPR reduction.

The performance comparison for all the PAPR reduction techniques described above are being shown in the table 3.1.

Table 3.1 Comparison of Different PAPR Reduction Techniques

Techniques	Distortion	Power increase	Data rate loss
Clipping and Filtering	Yes	No	No
Coding	No	No	Yes
Partial Transmit Sequence	No	No	Yes
Selected Mapping	No	No	Yes
Tone Reservation	No	Yes	Yes
Tone Injection	No	Yes	No
ACE	No	Yes	No
Companding	No	Yes	No

3.4 Analysis of PAPR using CCDF

If Z is a random variable then the Cumulative Distribution Function (CDF) of z is defined as the probability of the event $\{Z \leq z\}$. So the Complementary Cumulative Distribution Function is defined as the probability of the event $\{Z > z\}$.The complementary cumulative density function (CCDF) is the probability that PAPR exceeds some threshold value. CCDF plot is used to measure the PAPR performance of PAPR reduction technique.Let us consider x is the transmitted FBMC signal then from [7] then the theoretical CCDF of PAPR means the probability of the event $\{PAPR\{x\} > PAPR_0\}$ is given as

$$Pr\,(PAPR\{x\} > PAPR_0) = 1 - (1 - e^{-PAPR_0})^N \quad (13)$$

Where N is the number of sub-carriers. However for the discrete-time baseband signal x [n] the PAPR may not be same as that for the continuous-time baseband signal x (t).

In practice, the PAPR for the continuous-time signal can be measured only after implementing the actual hardware. So the PAPR can be estimated in some way from the discrete-time signal x [n]..It is realized that x [n] can show practically the same PAPR as x (t) if it is interpolated (oversampled) U times. Where $U \geq 4$ [1].For the oversampled signal the approximate value of the CCDF is given as

$$\Pr(\text{PAPR}\{x\} > \text{PAPR}_0) = 1 - (1 - e^{-\text{PAPR}_0})^{\alpha N} \quad (14)$$

Where α has to be determined by fitting the theoretical CCDF into the actual one.

3.5 Results and discussion

Fig. 3.1 represents the CCDF plot for original FBMC signal in which number of sub-channels are taken as 64.

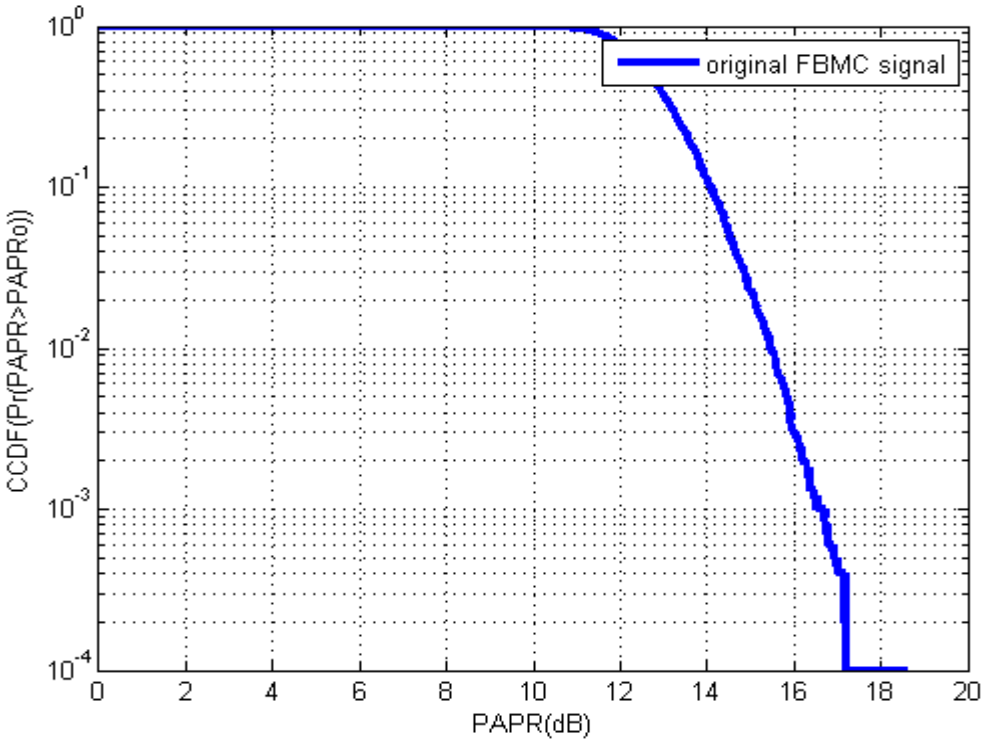

Fig.3.1 CCDF plot for Tone Injection technique

3.6 Tone Injection

The basic idea in tone injection technique is to increase the constellation size in such a way that each of the points in the original basic constellation can be mapped into several equivalent points in the expanded constellation [15]. Since each symbol in a data block can be mapped into one of the several equivalent points, these extra degrees of freedom can be used for PAPR reduction.

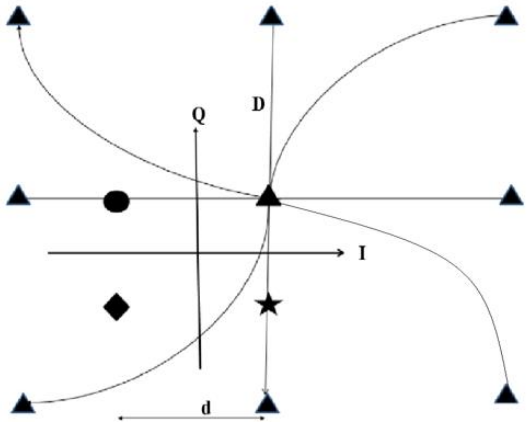

Fig. 3.2 cyclically extended 4-QAM constellation diagram.

In this method, one tone is injected with proper phase and frequency in the symbol that corresponds to adding one of these equivalent points with original constellation point. Hence, these additional constellation points can be used to generate FBMC symbols with low PAPR.

Fig. 4.1 illustrate the extended constellation for 4-QAM, where one point in the original constellation can be replaced by any one of its equivalent point. These equivalent points are spaced in real and/or imaginary axes by the extension size D. So, any one of the nine equivalent points can be used to obtain signals with lower PAPR. If, for an M-ary QAM, d is the minimum distance between signal points, constant D must be equal to or larger than $d\sqrt{M}$, so that adding equivalent constellation point does not increase BER.

Adding these equivalent constellation points to the original constellation point has an effect of increasing the transmitted power. However, probability that very large peaks occur is very less so overall average power will not increase significantly due to these tone modifications. After tone injection, the modified transmit signal is given by

$$s^*[n] = s[n] + c[n] \tag{15}$$

$$= \frac{1}{\sqrt{N}} \sum_{k=0}^{N-1} (S_k + C_k) e^{j2\pi kn/N} \tag{16}$$

Where the extension vector C_k is defined as

$$C_k = D(p_k + jq_k) \quad (17)$$

Where p_k and q_k take values from the set {1, 0, 1} to get any one of the extension constellation point. However, our problem is to find the optimal values of p_k and q_k, which will give lowest PAPR for s[n]. Here we used TI with aggressive clipping projection (TI-ACP) to achieve a very good and fast, suboptimal solution for finding preferred subcarriers and extension vectors for tone injection.

A clipped signal sclip[n] is defined

s_{clip}[n]=s[n]+c_{clip}[n] (18)

Where $c_{clip}[n]$ represents the clipped off portion of the signal. In the, Cclip[k] is the frequency domain representation of $c_{clip}[n]$. To obtain the peak reduction signal c[n], $C_{clip}[k]$ is projected on to the extension vectors to determine C_k in (12).The iterative signal can be given as

$$s^{i+1}[n] = s^i[n] + c[n] \quad (19)$$

Exact extension direction can be determined by $C_{clip}[k]$, and the extension vector is Chosen to be the projection with the largest magnitude. Extension vector Ck contains the largest magnitude vector among all the projected vectors, projecting onto the allowable extension vectors. Values of pk and qk in (13) can be given by

$$p_k = sgn(Re(C_{clip}[k])) \quad (20)$$

$$q_k = sgn(Im(C_{clip}[k])) \quad (21)$$

Where sgn represents the signum function. For single-tone modification, maximum possible peak reduction can be given as

$$|s[n]| - |s^*[n]| \le |c[n]| \quad (22)$$

$$= \left| \frac{D}{\sqrt{N}} (p_k + jq_k) e^{j2\pi kn/N} \right| \quad (23)$$

$$= \frac{D}{\sqrt{N}} \sqrt{p_k^2 + q_k^2} \quad (24)$$

For the complex baseband signal maximum peak reduction per tone injection can be achieved by choosing $|p_k| = 1$ and $|q_k| = 1$, which is given by

$$\delta_{max} = \frac{D}{\sqrt{N}} \sqrt{2} \quad (25)$$

Secondary peaks may grow for some values of pk and qk, above the current peak level, which can increase PAPR value of the signal. For a single-tone injection δ_{max} is also the maximum possible growth for a time-sample magnitude. So at each iteration, samples which exceed 2 δ_{max} below the largest peak level in magnitude is thus sufficient to consider because only these samples can cause an increase in PAPR.

3.6.1 The TI-ACP Algorithm

1. To get $c_{clip}[n]$ all $|s^i[n]| \geq A$ in magnitude is clipped

$$c_{clip}[n] = \begin{cases} 0 & |s^i[n]| \leq A \\ (A - |s^i[n]|)e^{j\theta[n]} & |s^i[n]| \geq A \end{cases} \quad (26)$$

   Where A is clipping level and

$$s[n] = |s[n]|e^{j\theta[n]} \quad (27)$$

2. Obtain Cclip via an FFT applied to c_{clip}.
3. Select the extension vector C_k for each subcarrier by projecting C_{clip} onto the allowable extension directions.
4. Find Ei, the largest-magnitude sample

$$E^i = \max_n |s^i[n]| \quad (28)$$

5. Find the sub-carrier k_1 which gives the maximum peak reduction

$$k_1 = \min_k |s_1[n_1]|^2 \quad (29)$$

   Where

$$s_1[n] = \begin{cases} 0 & |s^i[n]| < E^i - 2\delta_{max} \\ s^i[n] + \frac{1}{\sqrt{N}} C_k e^{j2\pi kn/N}, & |s^i[n]| \geq E^i - 2\delta_{max} \end{cases} \quad (30)$$

   and n1 is the peak point.

6. Compute

$$s^{i+1}[n] = s^i[n] + c[n] \quad (31)$$

   Where

$$c[n] = \frac{1}{\sqrt{N}} C_{k_1} e^{j2\pi k_1 n/N} \quad (32)$$

7. Increase iteration index i by 1 and go to Step 2 unless we reach a maximum iteration count or we get an acceptable PAPR level. Otherwise, stop PAPR reduction.

3.6.2 Complexity Analysis

A typical c_{clip} includes a relatively small number of samples and computing $C_{clip}[k]$ directly from sinusoides may be less expensive rather than using the FFT algorithm for searching extension vector.In addition, s[n] in Step 6 has only a few nonzero samples, so for each tone injection this results in a rapid search for the best sub channel.in Step 7, without using the IFFT algorithm, c[n] can be computed from sinusoides to obtain xi+1[n], as we get the low PAPR signal after several tone injections. The projections on the permissible extension vectors are obtained by using an FFT at each iteration, which results in V(N logN) complexity for this algorithm. However, the Ck do not change greatly unless the location of the largest magnitude sample moves to another location after injection of a tone. On the other hand, δ_{max} is relatively small compared to E_i so that the largest peak location can change rarely. Thus, skipping the algorithm steps involving projection may save computation as long as E_i stays at the same location. So the performance of TI-ACP will compensate for the hardware and computational complexity for FBMC systems.

3.6.3 The Aggressive Clipping Level

The clip level A in (12) serves an important role in finding the preferred sub channels to achieve the desired PAPR level. Generally the extension vectors C_k are larger than $C_{clip}[k]$ in magnitude, which is considered as a quantization error and makes it impossible to achieve the clip level A. Also if A is chosen to be equal or close to the clip or saturation level of a power amplifier, secondary peaks may easily grow above this clip level, causing increase of PAPR and convergence problems. So we have to choose clip level A carefully.

3.6.4 Advantages and Disadvantages of Tone Injection

Like all other PAPR reduction techniques, Tone Injection also has a wide set of advantages and has a few serious drawbacks.

Advantages of Tone Injection Technique

Distortion less technique: TI technique doesn't distort the input signal. So no bit error rate (BER) performance degradation problem.

No data rate loss: In TI technique, no data rate loss problem occurs Unlike PTS, SLM or other technique.

Low complexity: In PTS and SLM technique, there are numbers of FFT blocks required for searching low PAPR data block but in case of TI technique only one FFT block is required at transmitter side. So this method has the advantage of low complexity.

PAPR reduction capability: TI is an iterative method which allows us to reduce PAPR further by increasing the number of iterations.

Disadvantages of Tone Injection Technique

Power increase: In TI technique we add peak reduction signal with the original signal to reduce PAPR. So this new signal increases the average power level. Although the increase in power is only a small fraction of original signal.

3.7 COMPANDING

Companding term made from compression and expanding[16]. So in this technique compression and expansion of low and high amplitude signal is used to reduce PAPR.

Companding are of two types- linear and non-linear.

Linear Companding- In linear companding, only low amplitude signals are expanded. Here companding curve is a straight line.

Nonlinear companding- In nonlinear companding, low amplitude signals are expanded and high amplitude signals are compressed to obtain uniform distribution of the signal [19].

There are different types of linear and nonlinear companding, among them A-law and μ-law companding are mostly used.

μ-law companding: This is a standard technique for companding in U.S. and japan. Mathematical equation for μ-law companding at the transmitter side is given as

$$F(x)=\operatorname{sgn}(x)\ln(1+\mu|x|)/\ln(1+\mu), -1 \le x \le 1 \quad (33)$$

Where μ is the companding parameter (μ =255 is used, as it is the accepted U.S. and Japan standard for voice compander). Inverse companding at the receiver side is performed to get back the original signal. Mathematical equation for μ-law companding at the receiver side is given as

$$F^{-1}(y)=\operatorname{sgn}(y)\left(\frac{1}{\mu}\right)((1+\mu)^{|y|}-1), -1 \le y \le 1 \quad (34)$$

A-law companding: This is a standard technique for companding in Europe. Mathematical equation for A -law companding is given as

$$|y| = \begin{cases} \dfrac{1+\log(A|x|)}{1+\log A} & \dfrac{1}{A} \le |x| \le 1 \\ \dfrac{A|x|}{1+\log A} & 0 \le |m| \le \dfrac{1}{A} \end{cases}$$

Where A is the compression parameter (A=87.6 in Europe).

Chapter 4

ANALYSIS OF PAPR REDUCTION

4

ANALYSIS OF PAPR REDUCTION

4.1 TI and Companding based PAPR Reduction of FBMC-FMT System

Tone injection (TI) and companding are two technique for PAPR reduction discussed in previous chapter. Here we present a new scheme of PAPR reduction by combining these two techniques for FBMC-FMT system, where FBMC signal is generated by using FMT method. Transmitter and receiver sections are designed for above scheme with prototype filter based on Blackman-Harris window and PHYDYAS filter.

4.1.1 Prototype filter design

Prototype filter for FBMC-OQAM system is designed by using a windowing technique with PHYDYAS filter[4]. Blackman-Harris window is taken as a window function because it gives around 90 dB sidelobe reduction. Blackman-Harris window is given by

$$w(n) = 0.35875 - 0.48829\cos\left(\frac{2\pi n}{N-1}\right) + 0.14128\cos\left(\frac{4\pi n}{N-1}\right) - 0.01168\cos\left(\frac{6\pi n}{N-1}\right) \quad (35)$$

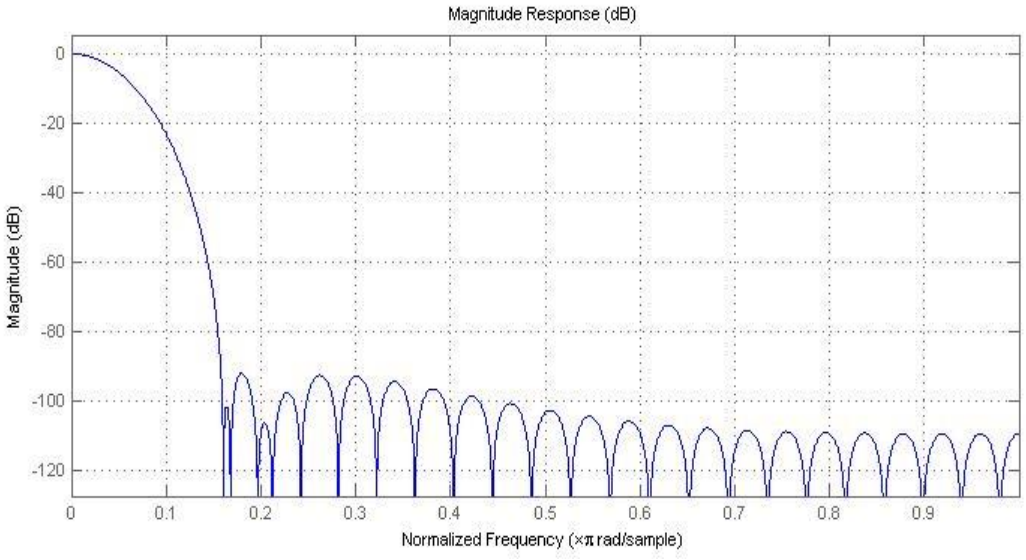

Fig. 4.1 Frequency response of prototype filter using Blackman-Harris window.

PHYDYAS filter was originally designed by Bellanger [4] and later it was chosen to be the reference prototype filter of the European project PHYDYAS The impulse response of the PHYDYAS filter is given as

$$h(t) = \begin{cases} \frac{1}{\sqrt{A}}[1+2\sum_{k=1}^{K-1}(-1)^k H_k cos(\frac{2\pi kt}{KT})] & t \in [0, KT] \\ 0 & elsewhere \end{cases} \quad (36)$$

Where A is normalization constant

$$A = KT\left[1+2\sum_{k=1}^{K-1} H_k^2\right] \quad (37)$$

In our filter, filter coefficients for PHYDYAS filter are calculated by using Blackman-harris window technique to reduce out of band radiation. Transmitter and receiver sections are explained below.

4.1.2 Transmitter

Fig. 4.2 shows the block diagram of FBMC-FMT System, which consist of transmitter and receiver sections. In the transmitter section first QAM modulated complex input signal is converted from serial to parallel. Then this parallel data stream is given to weighted frequency spreading block, which spread each data element into 2K-1 sub-carriers and also filter input data element. Where K is overlapping factor. After that parallel data stream is given to IFFT block for the generation of FBMC-FMT signal. Size of IFFT block is (2K-1)N. Where N is number of sub-channels. Then this IFFT output is converted from parallel to serial to get the FBMC-FMT signal. After the generation of FBMC signal it is processed to reduce PAPR of the signal. For PAPR reduction here a combined scheme of tone injection and companding techniques is used. In this scheme FBMC signal is first given to compander block for expansion of low amplitude signal and compression of high amplitude signal. Here μ–law companding is used as a companding technique. After companding this signal is given to tone injection part, where a PAPR reduction signal is added to the main signal with each tone injection. Tone injection is an iterative method, so we can further reduce PAPR of the FBMC signal by increasing the number of iterations. After this FBMC signal with reduced PAPR is converted from digital to analog by using digital to analog converter for transmission through channel.

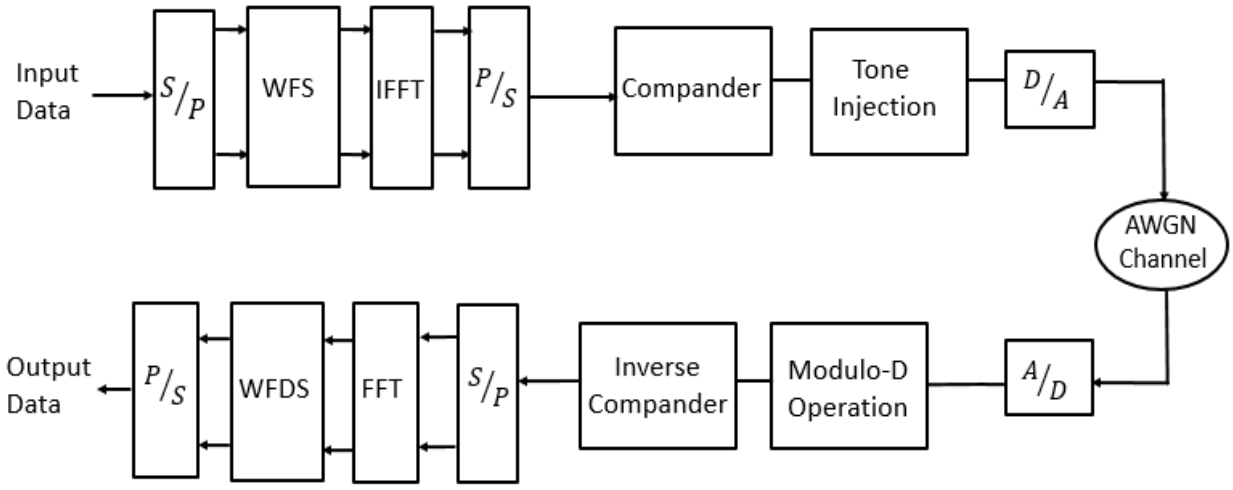

Fig. 4.2 Block Diagram of FBMC-FMT System with proposed scheme

4.1.3 Receiver

In the receiver section, signal from transmitter is received through AWGN channel. This received signal is first converted from analog to digital by using A/D converter so that it can be given to digital processor for demodulation of signal. After analog to digital conversion signal is given to modulo-D block, where injected tones are removed from FBMC signal by using modulo-D operation. Then this signal is given to inverse compander block, where inverse operation of compander block is performed to back the original FBMC signal. Then this FBMC signal is converted from serial to parallel and then pass through FFT block for demodulation of FBMC signal. Then this signal is pass through weighted frequency dispreading block, where spreaded data is filtered and added up to get the original data element. After this data elements are converted from parallel to serial to get back the original input data stream.

4.1.4 Results and Discussion

Simulation is performed for FBMC-FMT system with 4-QAM and 16-QAM modulated input signals. Number of sub-channels are N=64 and overlapping factor is taken as K=4. Tone injection, μ-law companding and combined scheme of these two techniques are used as a PAPR reduction technique. Clipping level A is chosen to be 3 dB above average power. For simulation 10^4 randomly generated complex input symbols are taken. Fig. 4.3 represents the CCDF plot for original FBMC-FMT signal, companding and tone injection with 3 iterations for 4-QAM input signal. Fig. 4.4 represents CCDF plot for original FBMC-FMT signal and combined scheme of tone injection and companding for 3 iterations for 4-QAM input signal. Comparing these two plots we can conclude that by combining TI and companding techniques PAPR performance improves significantly. Fig. 4.5 represents the CCDF plot for original FBMC-

FMT signal, companding and tone injection with 3 iterations for 16-QAM input signal. Fig. 4.6 represents CCDF plot for original FBMC-FMT signal and combined scheme of tone injection and companding for 3 iterations for 16-QAM input signal. PAPR performance improvement for 16-QAM modulated signal is same as for 4-QAM modulation. PAPR performance improves as we move from 4-QAM to 16-QAM.

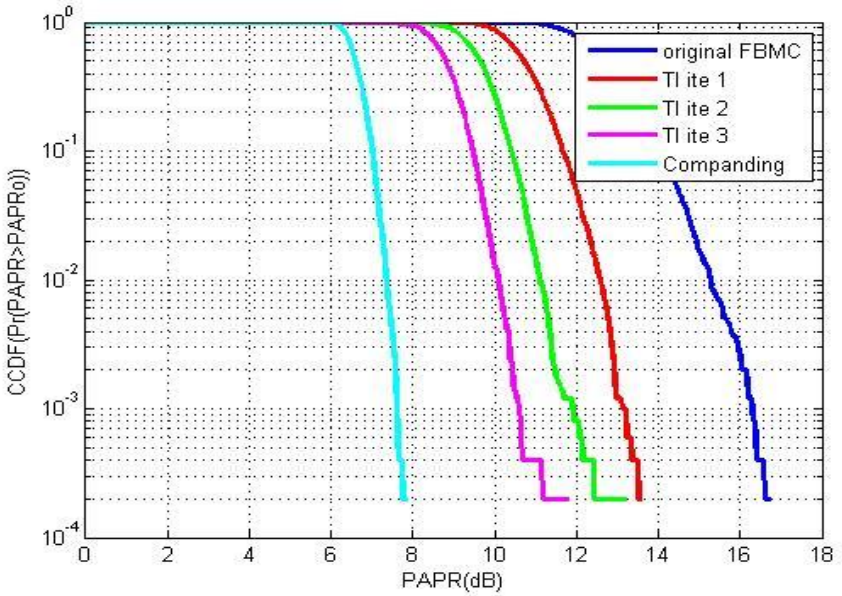

Fig. 4.3 CCDF plot for original FBMC-FMT signal, TI and Companding techniques (4-QAM).

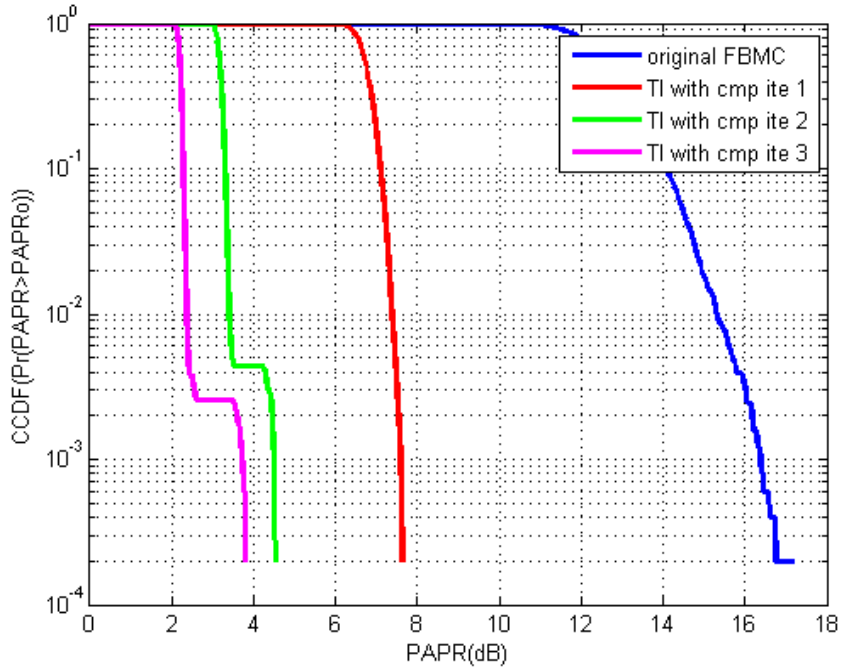

Fig. 4.4 CCDF plot for original FBMC-FMT signal and combined scheme of TI and Companding techniques for 3 iterations (4-QAM).

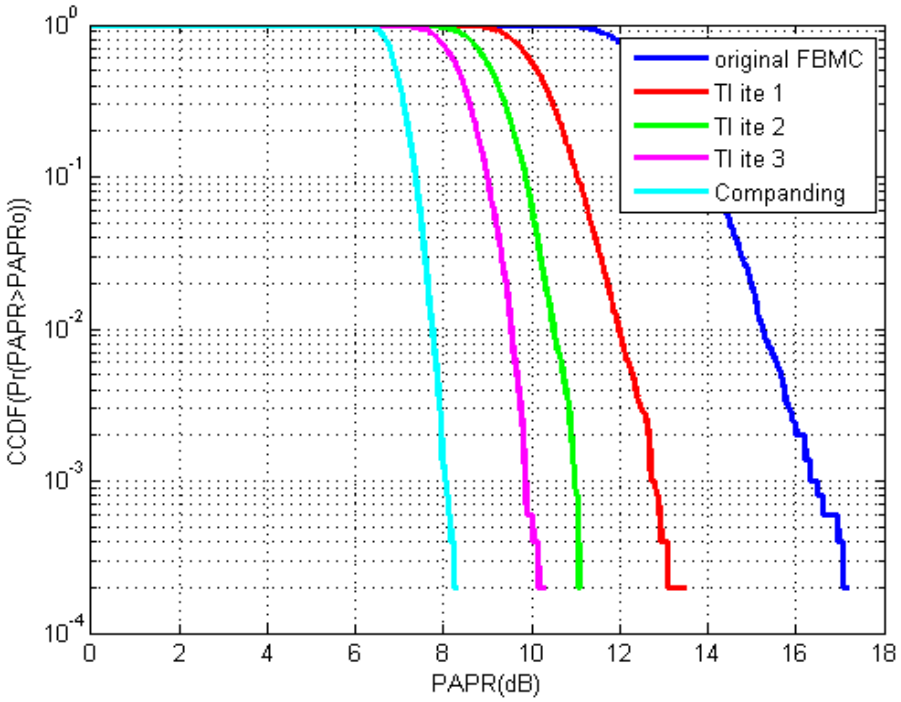

Fig. 4.5 CCDF plot for original FBMC-FMT signal, TI and Companding techniques (16-QAM).

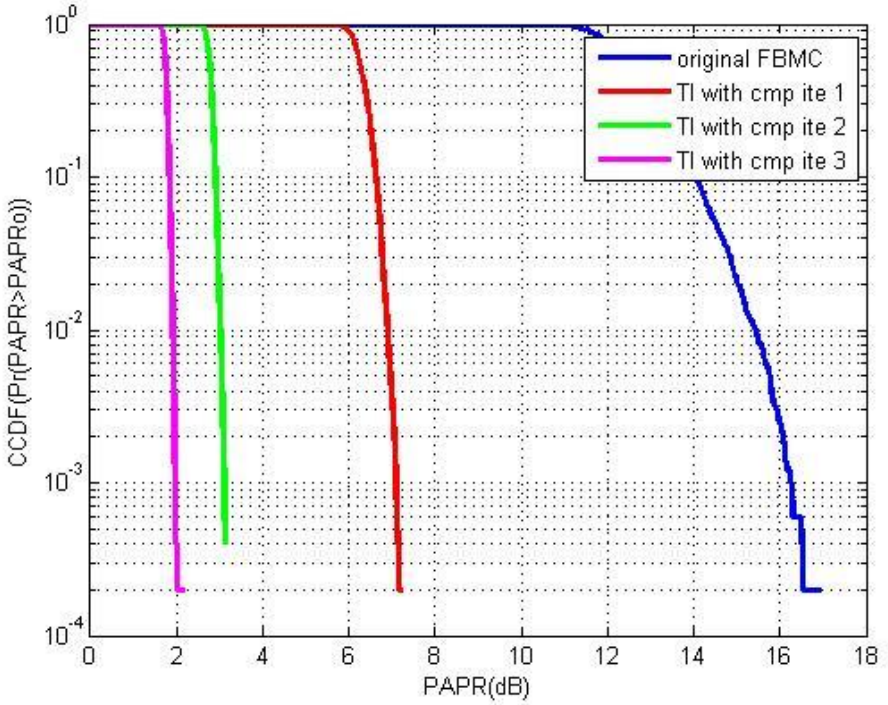

Fig. 4.6 CCDF plot for original FBMC-FMT signal and combined scheme of TI and Companding techniques for 3 iterations (16-QAM).

4.1.5 Power Amplifier (PA) Efficiency Calculation

Operating point of PA should be adjusted to the average input power of the multicarrier signal in order to avoid clipping[17]. An input back-off (IBO) is required in PA prior to amplification so that the input signal in the PA do not get distorted. The required amount of the IBO is closely related to the PAPR. For a linear class A amplifier, the PA efficiency η and the PAPR are related by $\eta = \frac{\eta_{\max}}{PAPR}$ where $\eta_{\max}$ = 0.5 for an ideal class A amplifier.

Table 4.1 contains PAPR values for different PAPR reduction technique and original FBMC signal for 10^{-3} clip probability and efficiency of PA for different PAPR reduction techniques.

Table 4.1 PAPR and efficiency comparison for FBMC-FMT system

	PAPR(dB) (4-QAM)	η (4-QAM)	PAPR(dB) (16-QAM)	η (16-QAM)
Original FBMC-FMT signal	16.3	1.17	16.2	1.2
Tone Injection, iteration 1	13.3	2.39	12.8	2.62
Tone Injection, iteration 2	12	3.16	11	3.97
Tone Injection, iteration 3	10.5	4.46	9.9	5.12
μ-law companding	7.7	8.49	8	7.92
Tone Injection with companding, iteration 1	7.7	8.49	7.1	9.75
Tone Injection with companding, iteration 2	4.6	17.34	3.3	22.39
Tone Injection with companding, iteration 3	3.8	20.85	2	31.55

From the above table we can conclude that there is significant performance improvement in PAPR and efficiency by combined scheme and also some improvement in performance for 16-QAM compared to 4-QAM.

4.2 TI and Companding based PAPR Reduction of FBMC-SMT System

Tone injection (TI) and companding are two technique for PAPR reduction discussed in previous chapter. Here we present a new scheme of PAPR reduction by combining these two techniques for FBMC-SMT system, where FBMC signal is generated by using SMT method. Transmitter and receiver sections are designed for above scheme with prototype filter based on Blackman-Harris window and PHYDYAS filter.

4.2.1Prototype filter design

Prototype filter for FBMC-OQAM system is designed by using a windowing technique with PHYDYAS filter[4]. Which is shown in previous section.

4.2.2 Transmitter

Fig. 4.7 shows the block diagram of FBMC-SMT System, which consist of transmitter and receiver sections. In the transmitter section first QAM modulated complex input signal is converted from serial to parallel. Then this parallel data stream is given to OQAM pre-processing block, where QAM signal is converted into offset QAM for the generation of SMT signal. Then this parallel data stream from OQAM pre-processing block is given to weighted frequency spreading block, which spread each data element into 2K-1 sub-carriers and also filter input data element. Where K is overlapping factor. After that parallel data stream is given to IFFT block for the generation of FBMC-FMT signal. Size of IFFT block is KN. Where N is number of sub-channels. Then this IFFT output is converted from parallel to serial to get the FBMC-SMT signal. After the generation of FBMC signal it is processed to reduce PAPR of the signal. For PAPR reduction here a combined scheme of tone injection and companding techniques is used. In this scheme FBMC signal is first given to compander block for expansion of low amplitude signal and compression of high amplitude signal. Here μ–law companding is used as a companding technique. After companding this signal is given to tone injection part, where a PAPR reduction signal is added to the main signal with each tone injection. Tone injection is an iterative method, so we can further reduce PAPR of the FBMC signal by increasing the number of iterations. After this FBMC signal with reduced PAPR is converted from digital to analog by using digital to analog converter for transmission through channel.

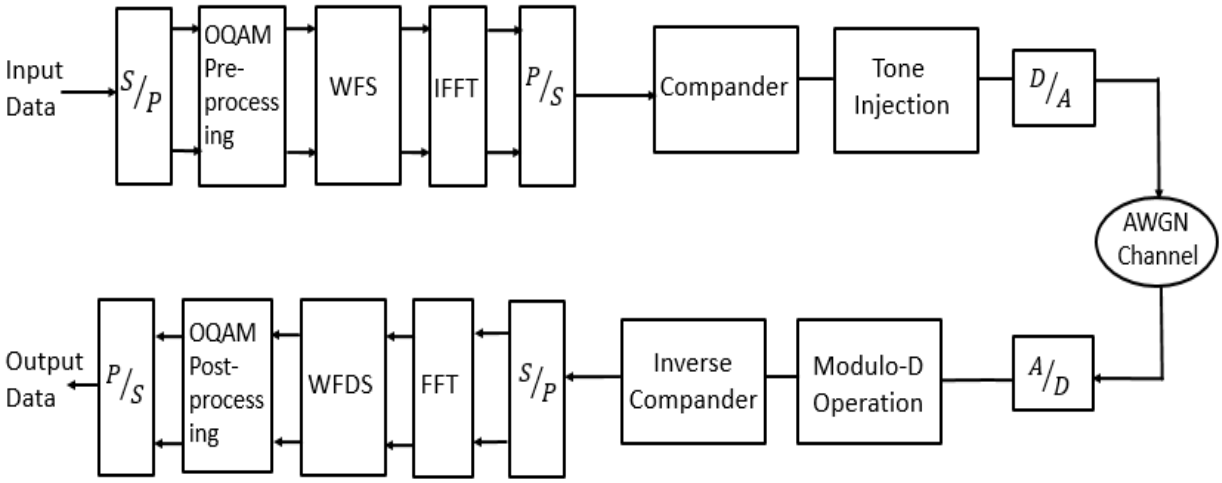

Fig. 4.7 Block Diagram of FBMC-SMT System with proposed scheme

4.2.3 Receiver

In the receiver section, signal from transmitter is received through AWGN channel. This received signal is first converted from analog to digital by using A/D converter so that it can be given to digital processor for demodulation of signal. After analog to digital conversion signal is given to modulo-D block, where injected tones are removed from FBMC signal by using modulo-D operation. Then this signal is given to inverse compander block, where inverse operation of compander block is performed to back the original FBMC signal. Then this FBMC signal is converted from serial to parallel and then pass through FFT block for demodulation of FBMC signal. Then this signal is pass through weighted frequency dispreading block, where spreaded data is filtered and added up and pass through OQAM post processing block to get the original data element. After this data elements are converted from parallel to serial to get back the original input data stream.

4.2.4 Results and Discussion

Simulation is performed for FBMC-SMT system with 4-QAM and 16-QAM modulated input signals. Number of sub-channels are N=64 and overlapping factor is taken as K=4. Tone injection, μ-law companding and combined scheme of these two techniques are used as a PAPR reduction technique. Clipping level A is chosen to be 3 dB above average power. For simulation 10^4 randomly generated complex input symbols are taken. Fig.4.8 represents the CCDF plot for original FBMC-SMT signal, companding and tone injection with 3 iterations for 4-QAM input signal. Fig. 4.9 represents CCDF plot for original FBMC-SMT signal and combined scheme of tone injection and companding for 3 iterations for 4-QAM input signal. Comparing

these two plots we can conclude that by combining TI and companding techniques PAPR performance improves significantly. Fig. 4.10 represents the CCDF plot for original FBMC-SMT signal, companding and tone injection with 3 iterations for 16-QAM input signal. Fig. 4.11 represents CCDF plot for original FBMC-SMT signal and combined scheme of tone injection and companding for 3 iterations for 16-QAM input signal. PAPR performance improvement for 16-QAM modulated signal is same as for 4-QAM modulation. PAPR performance improves as we move from 4-QAM to 16-QAM. Fig. 4.12 represents the SER plot for for original FBMC-SMT signal, tone injection, companding technique and combined scheme of tone injection and companding for 4-QAM input signal. It shows that SER performance of combined scheme is better compared to companding and tone injection techniques but some degradation in performance occurs compared to original FBMC-SMT signal.

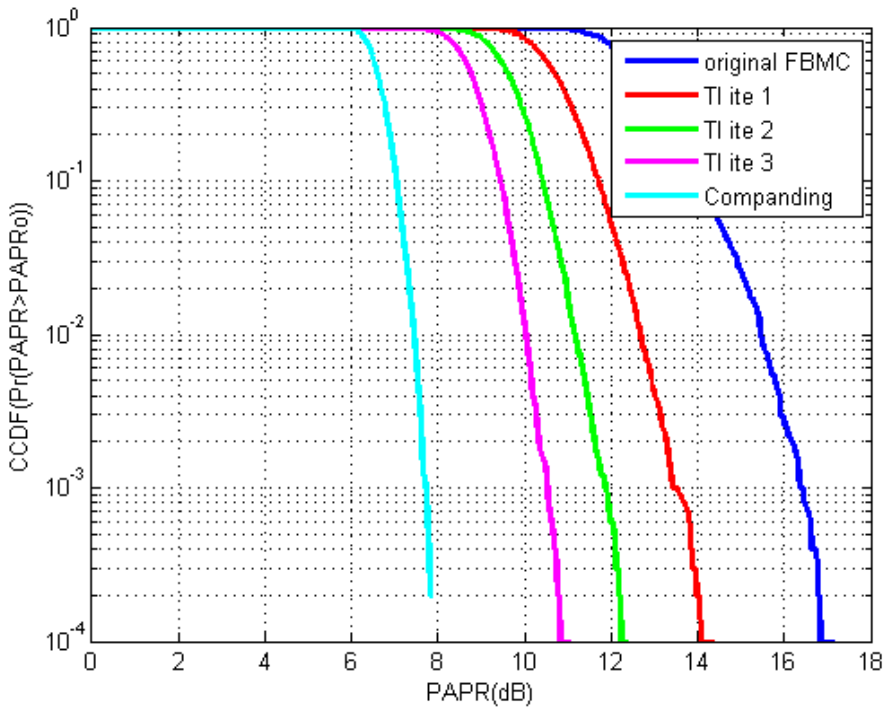

Fig. 4.8 CCDF plot for original FBMC-SMT signal, TI and Companding techniques (4-QAM).

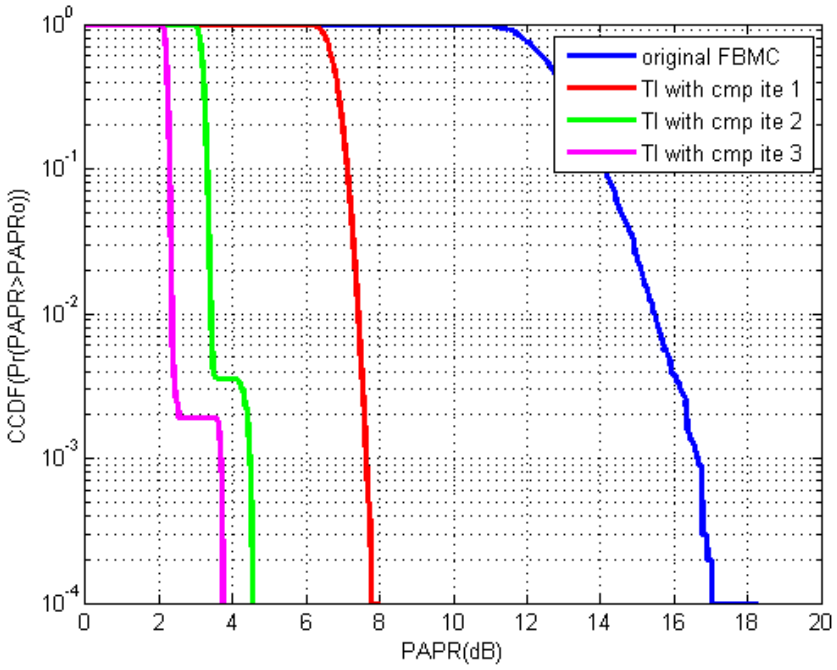

Fig. 4.9 CCDF plot for original FBMC-SMT signal and combined scheme of TI and Companding techniques with 3 iterations (4-QAM)

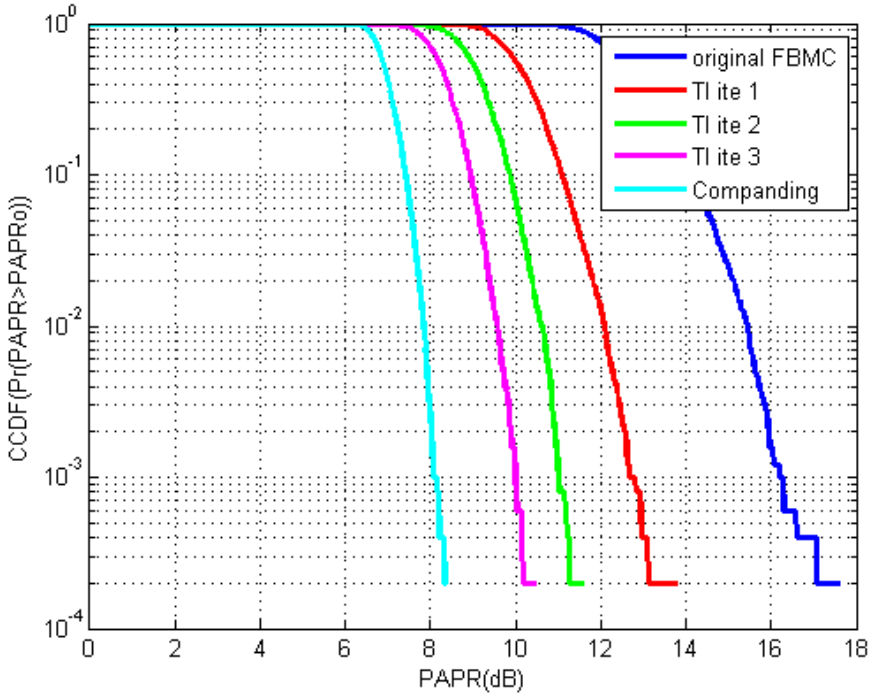

Fig. 4.10 CCDF plot for original FBMC-SMT signal, TI and Companding techniques (16-QAM).

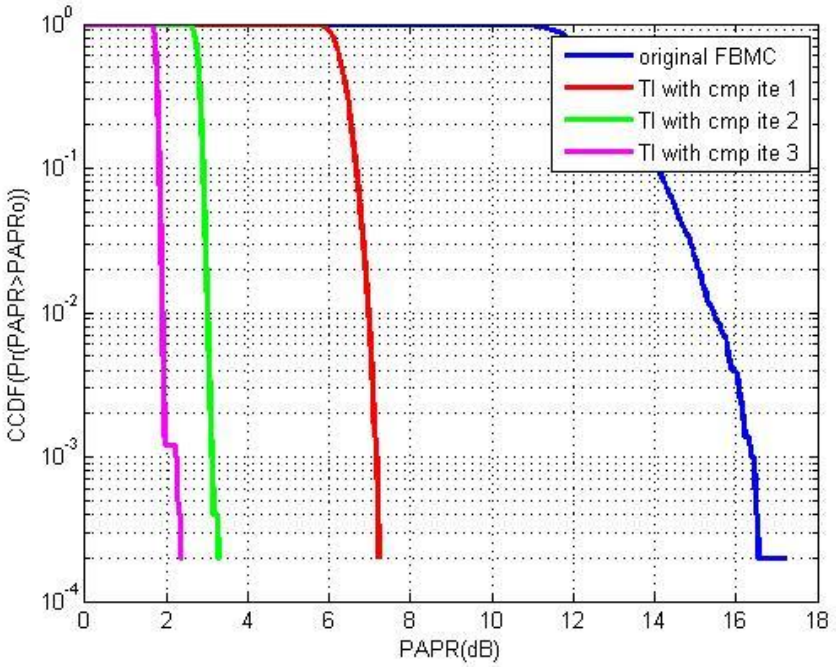

Fig. 4.11 CCDF plot for original FBMC-SMT signal and combined scheme of TI and Companding techniques with 3 iterations (16-QAM).

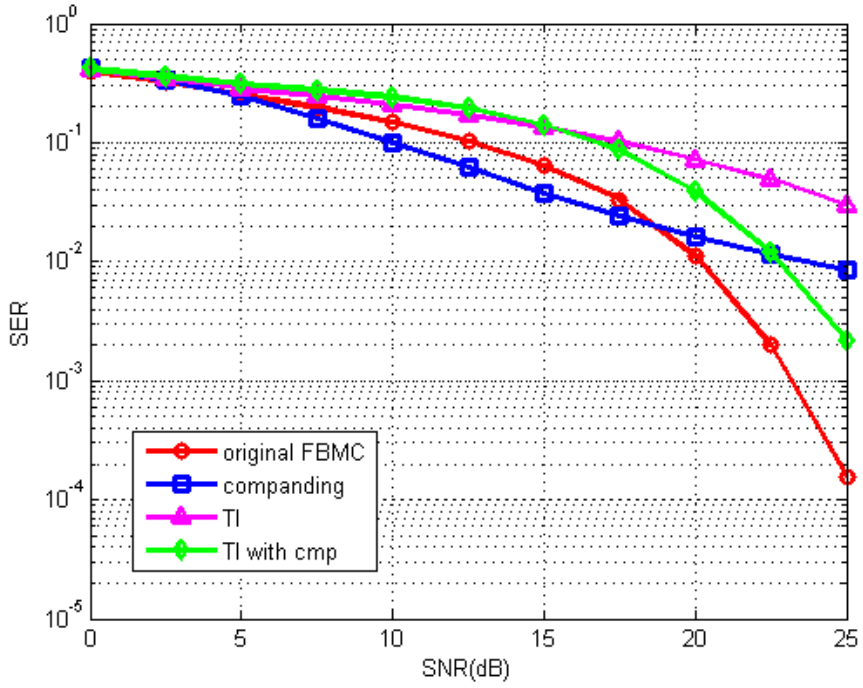

Fig. 4.12 BER Plot for original FBMC-SMT, companding and combined scheme for 4-QAM.

4.2.5 Power Amplifier (PA) Efficiency Calculation

Table 4.2 contains PAPR values for different PAPR reduction technique and original FBMC signal for 10^{-3} clip probability and efficiency of PA for different PAPR reduction techniques.

Table 4.2 PAPR and efficiency comparison for FBMC-SMT system

	PAPR(dB) (4-QAM)	η (4-QAM)	PAPR(dB) (16-QAM)	η (16-QAM)
Original FBMC-SMT signal	16.4	1.15	16.2	1.2
Tone Injection, iteration 1	13.4	2.29	12.8	2.62
Tone Injection, iteration 2	11.9	3.23	11.1	3.88
Tone Injection, iteration 3	10.5	4.46	10	5
μ-law companding	7.7	8.49	8.1	7.74
Tone Injection with companding, iteration 1	7.8	8.28	7.2	9.5
Tone Injection with companding, iteration 2	4.5	17.74	3.3	23.39
Tone Injection with companding, iteration 3	3.7	21.33	2.1	30.83

From the above table we can conclude that there is significant performance improvement in PAPR and efficiency by combined scheme and also some improvement in performance for 16-QAM compared to 4-QAM.

4.3 New Clipping based PAPR Reduction Scheme for FBMC System

In the clipping technique of PAPR reduction, signal is just clipped off above a predefined clipping level. So in this technique, signal portion is removed permanently and can not be recovered at the receiver section. These bits increase bit error and BER performance of the system degraded [18].

In the proposed technique, clipped portion is modulated and transmitted with the clipped signal instead of permanently removing it. At the receiver side these two portion can be separated by proper filtering and added together to get back the original signal. In this way we can

significantly reduce the PAPR of the signal without degrading BER performance much. This technique can be applied for PAPR reduction of FBMC system. New clipping based PAPR reduction scheme for FBMC signal generated by CMT, FMT, and SMT methods are discussed below.

4.3.1 FBMC-CMT

In the CMT method of FBMC signal generation synthesis filter bank at the transmitter and analysis filter bank at the receiver is used for generation of FBMC signal. Here prototype filter based on Blackman-Harris window technique is used.

Synthesis filter bank design

For prototype filter $h_p(n)$, synthesis filter $f_k(n)$ is given as

$$f_k(n) = 2h_p(n)\cos((2k+1)\frac{\pi}{2M}(n-\frac{N}{2}) - \phi_k$$

Where M is number of sub-channels and N is the length of prototype filter. ϕ_k must be chosen as ϕ_k =$(-1)^k$ π/4, k=0, 1...M-1.

Analysis filter bank design

For prototype filter $h_p(n)$, analysis filter $h_k(n)$ is given as

$$h_k(n) = 2h_p(n)\cos((2k+1)\frac{\pi}{2M}(n-\frac{N}{2}) + \phi_k$$

4.3.1.1 Transmitter

Fig.4.13 shows the block diagram of transmitter and receiver section for proposed scheme. In the transmitter section first input PAM signal is converted from serial to parallel. Then this parallel data stream is given to synthesis filter bank for generation of FBC signal. In synthesis filter bank first input signal is given to prototype filter and then modulated with cosine signal of different frequency to place the signal into different sub-channel and then added to get the FBMC signal. After the generation of FBMC signal it is processed to reduce PAPR of the signal. Here clipping based PAPR reduction technique is used for PAPR reduction of FBMC signal. For this FBMC signal is feed to peak cancellation signal generator block for generating peak cancellation signal. This peak cancellation signal is then subtracted from FBMC signal to clip the portion above clipping level and also this peak cancellation signal is modulated so that it can be added to the clipped FBMC signal without any interference. Then this modulated peak cancellation signal is added with the clipped FBMC signal and converted from digital to analog

by using digital to analog converter for transmission through channel.

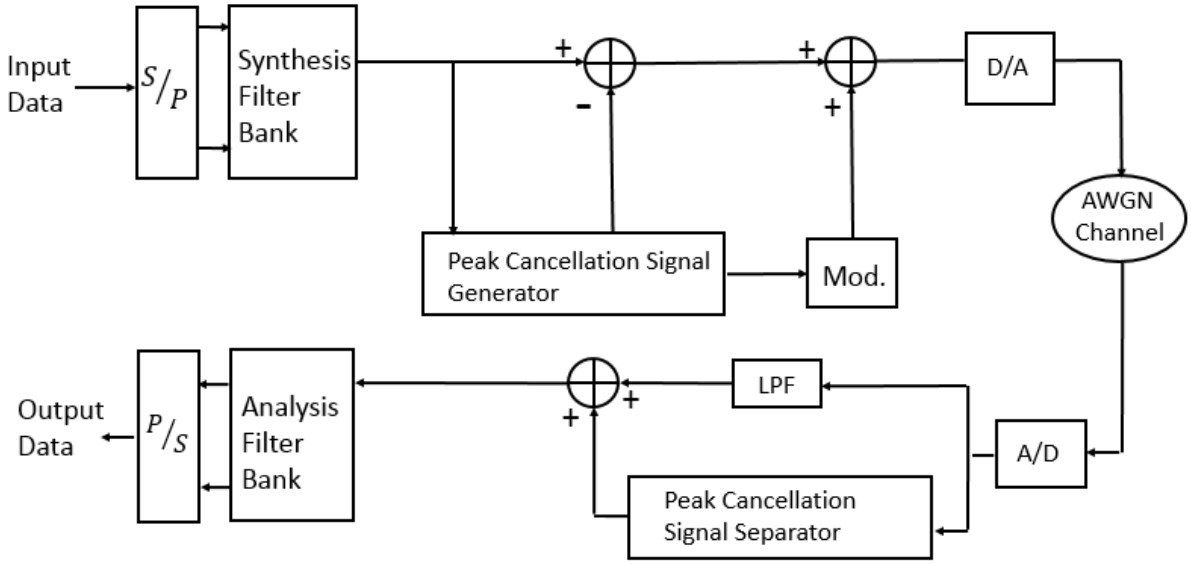

Fig. 4.13 Block Diagram of FBMC-CMT System with proposed scheme

4.3.1.2Receiver

In the receiver section, signal from transmitter is received through AWGN channel. This received signal is first converted from analog to digital by using A/D converter so that it can be given to digital processor for demodulation of signal. After analog to digital conversion signal is given to low pass filter and peak cancellation signal separator blocks to separate the clipped FBMC signal and peak cancellation signal. In the LPF block a low pass filter with a cut off frequency equal to the frequency of highest sub-channel is use. In the peak cancellation signal separator block after demodulation, we get peak cancellation signal and add this with filtered clipped signal to get back the original FBMC signal. This FBMC signal is then given to analysis filter block for recovering original data elements and then data elements are converted from parallel to serial to get back the original input data stream.

4.3.1.3 Results and Discussion

Simulation is performed for FBMC-CMT system with 4-PAM and 16-PAM modulated input signals. Number of sub-channels are N=64 and clipping level A is taken as 5 dB above the average power level. Fig. 4.14 show the CCDF plot for original FBMC-CMT, clipped signal and combined signal for 4-PAM modulated signal. Plot shows that PAPR performance improves significantly by clipping technique and combining clipped signal with peak cancellation signal reduces PAPR value by only small amount. Which can be tolerate as this signal gives higher BER performance compared to clipped signal. Fig. 4.15 show the CCDF plot for original FBMC-CMT, clipped signal and combined signal for 16-PAM modulated

signal. Comparing these plots we can say that there is some improvement in performance for 16-PAM compared to 4-PAM.

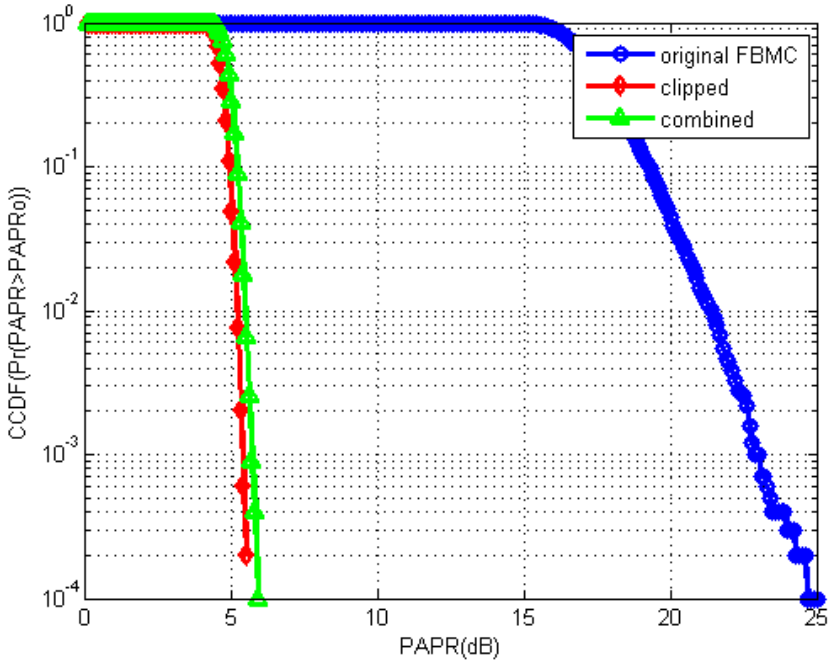

Fig. 4.14 CCDF Plot for original FBMC-CMT signal, clipped signal and combined signal (4-PAM).

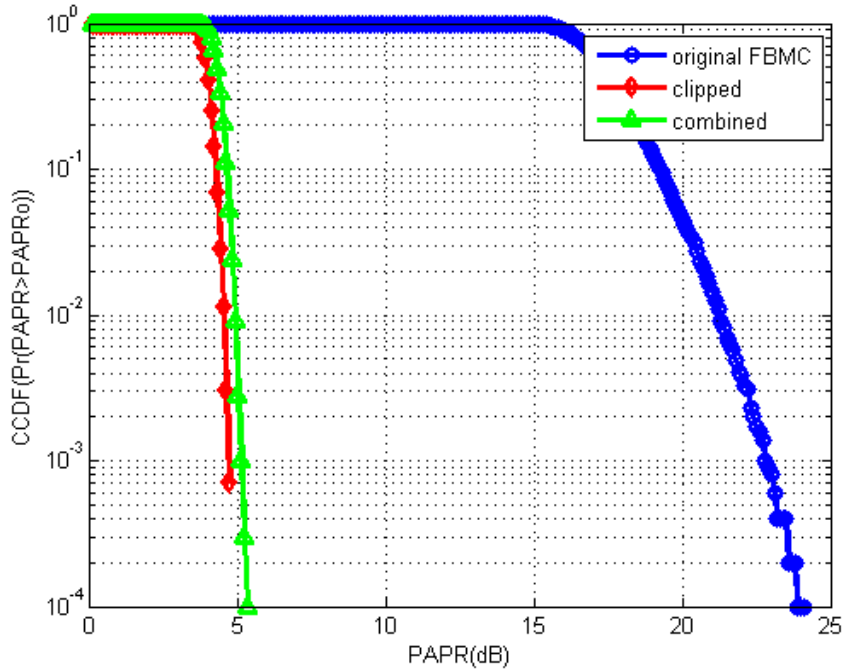

Fig. 4.15 CCDF Plot for original FBMC-CMT signal, clipped signal and combined signal (16-PAM).

4.3.1.4 Power Amplifier (PA) Efficiency Calculation

Table 4.3 contains PAPR values for different PAPR reduction technique and original FBMC signal for 10^{-3} clip probability and efficiency of PA for different PAPR reduction technique.

Table 4.3 PAPR and efficiency comparison for FBMC-CMT system with new clipping based PAPR reduction technique

	PAPR(dB) (4-PAM)	η (4-PAM)	PAPR(dB) (16-PAM)	η (16-PAM)
Original FBMC-CMT signal	22.8	0.26	22.6	0.2
Clipped signal	5.4	14.4	4.65	17.14
Clipped with peak cancellation signal	5.7	13.46	5	15.81

4.3.2 FBMC-SMT

Here we present a new clipping based PAPR reduction scheme for PAPR reduction of FBMC-SMT system, where FBMC signal is generated by using SMT method. Transmitter and receiver sections are designed for above scheme with prototype filter based on Blackman-Harris window and PHYDYAS filter.

4.3.2.1 Transmitter

Fig. 4.16 shows the block diagram of FBMC-SMT System, which consist of transmitter and receiver sections. In the transmitter section first QAM modulated complex input signal is converted from serial to parallel. Then this parallel data stream is given to OQAM pre-processing block, where QAM signal is converted into offset QAM for the generation of SMT signal. Then this parallel data stream from OQAM pre-processing block is given to weighted frequency spreading block, which spread each data element into 2K-1 sub-carriers and also filter input data element. Where K is overlapping factor. After that parallel data stream is given to IFFT block for the generation of FBMC-FMT signal. Size of IFFT block is KN. Where N is number of sub-channels. Then this IFFT output is converted from parallel to serial to get the FBMC-SMT signal. After the generation of FBMC signal it is processed to reduce PAPR of the signal. Here clipping based PAPR reduction technique is used for PAPR reduction of FBMC signal. For this FBMC signal is feed to peak cancellation signal generator block for generating peak cancellation signal. This peak cancellation signal is then subtracted from

FBMC signal to clip the portion above clipping level and also this peak cancellation signal is modulated so that it can be added to the clipped FBMC signal without any interference. Then this modulated peak cancellation signal is added with the clipped FBMC signal and converted from digital to analog by using digital to analog converter for transmission through channel.

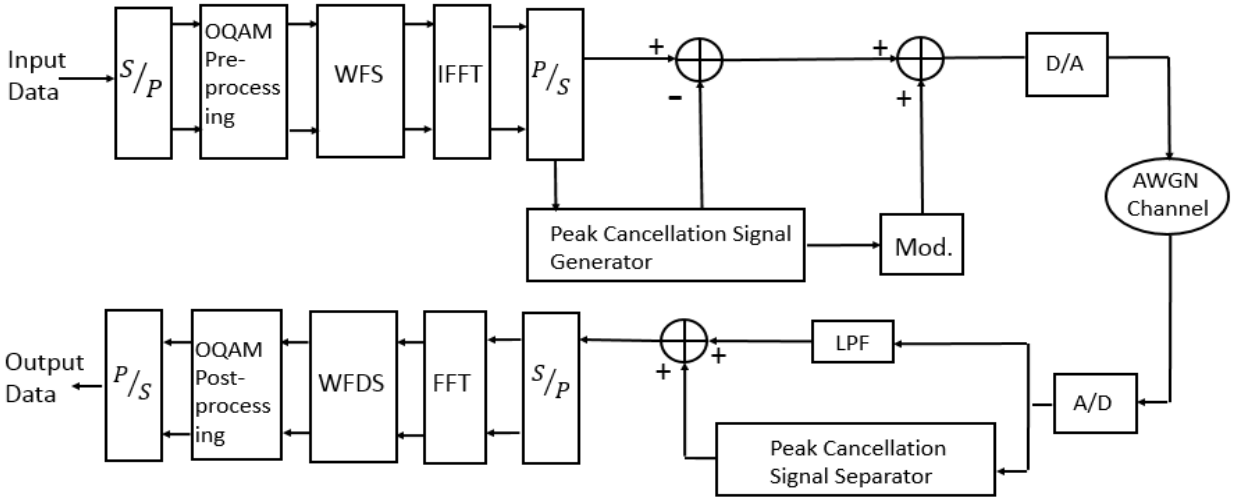

Fig. 4.16 Block Diagram of FBMC-SMT System with Proposed Scheme

4.3.2.2 Receiver

In the receiver section, signal from transmitter is received through AWGN channel. This received signal is first converted from analog to digital by using A/D converter so that it can be given to digital processor for demodulation of signal. After analog to digital conversion signal is given to low pass filter and peak cancellation signal separator blocks to separate the clipped FBMC signal and peak cancellation signal. In the LPF block a low pass filter with a cut off frequency equal to the frequency of highest sub-channel is use. In the peak cancellation signal separator block after demodulation, we get peak cancellation signal and add this with filtered clipped signal to get back the original FBMC signal. Then this FBMC signal is converted from serial to parallel and then pass through FFT block for demodulation of FBMC signal. Then this signal is pass through weighted frequency dispreading block, where spreaded data is filtered and added up and pass through OQAM post processing block to get the original data element. After this data elements are converted from parallel to serial to get back the original input data stream.

4.3.2.3 Results and Discussion

Simulation is performed for FBMC-SMT system with 4-QAM and 16-QAM modulated input signals. Number of sub-channels are N=64 and clipping level A is taken as 5 dB above the average power level. Fig. 4.17 show the CCDF plot for original FBMC-SMT, clipped signal and combined signal for 4-QAM modulated signal. Plot shows that PAPR performance improves significantly by clipping technique and combining clipped signal with peak cancellation signal reduces PAPR value by only small amount. Which can be tolerate as this signal gives higher BER performance compared to clipped signal. Fig. 4.18 show the CCDF plot for original FBMC-SMT, clipped signal and combined signal for 16-QAM modulated signal. Comparing these plots we can say that there is some improvement in performance for 16-QAM compared to 4-QAM.

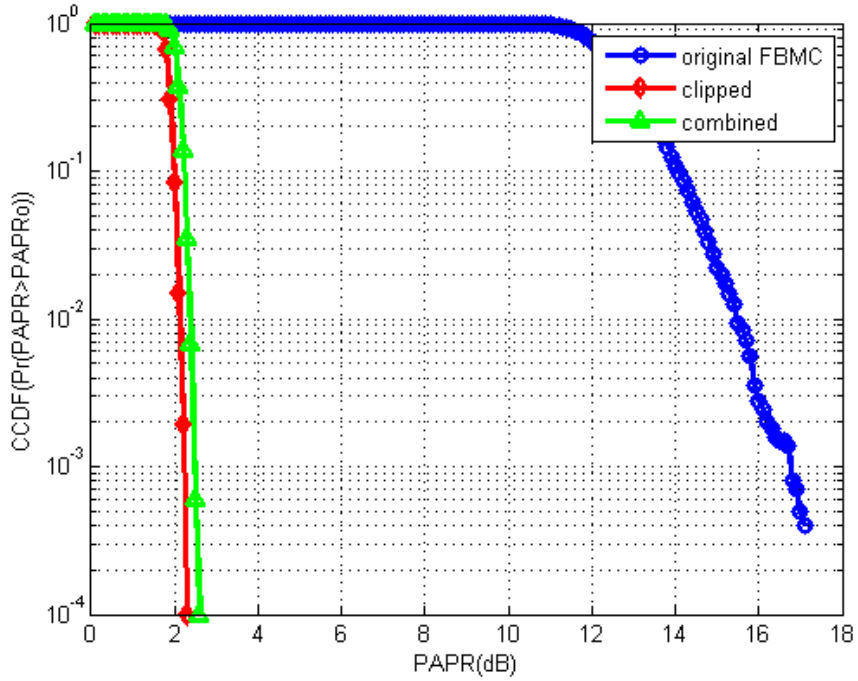

Fig. 4.17 CCDF Plot for original FBMC-SMT signal, clipped signal and combined signal (4-QAM).

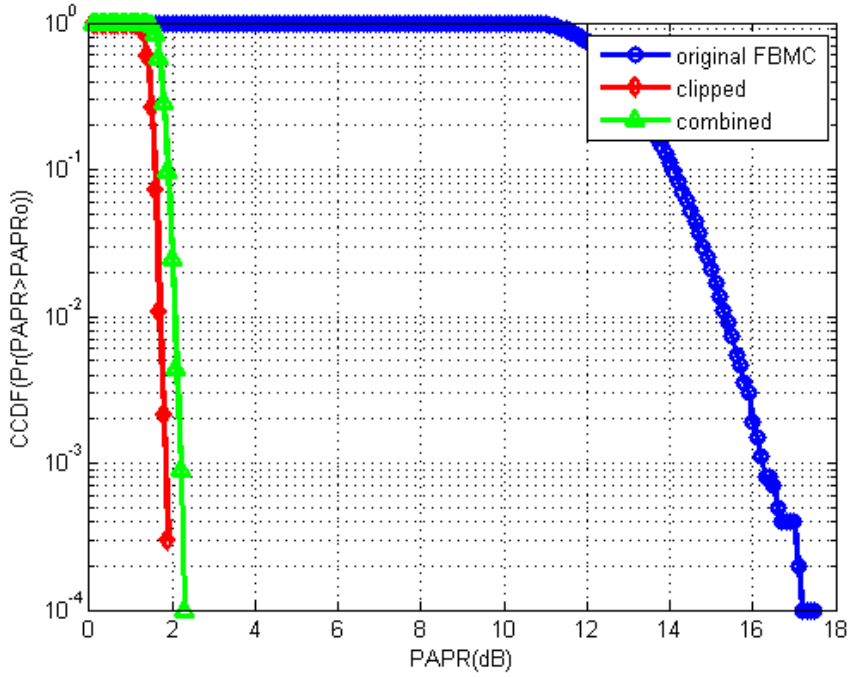

Fig. 4.18 CCDF Plot for original FBMC-SMT signal, clipped signal and combined signal (16- QAM).

4.3.2.4 Power Amplifier (PA) Efficiency Calculation

Table 4.4 contains PAPR values for different PAPR reduction technique and original FBMC signal for 10^{-3} clip probability and efficiency of PA for different PAPR reduction techniques.

Table 4.4 PAPR and efficiency comparison for FBMC-SMT system with new clipping based PAPR reduction technique

	PAPR(dB) (4-QAM)	η (4-QAM)	PAPR(dB) (16-QAM)	η (16-QAM)
Original FBMC-SMT signal	16.5	1.12	16.3	1.17
Clipped signal	2.25	29.78	1.85	32.66
Clipped with peak cancellation signal	2.55	27.80	2.05	31.19

4.3.3 FBMC-FMT

Here we present a new clipping based PAPR reduction scheme for PAPR reduction of FBMC-FMT system, where FBMC signal is generated by using FMT method. Transmitter and receiver sections are designed for above scheme with prototype filter based on Blackman-Harris window and PHYDYAS filter.

4.3.3.1 Transmitter

Fig. 4.19 shows the block diagram of FBMC-FMT System, which consist of transmitter and receiver sections. In the transmitter section first QAM modulated complex input signal is converted from serial to parallel. Then this parallel data stream is given to weighted frequency spreading block, which spread each data element into 2K-1 sub-carriers and also filter input data element. Where K is overlapping factor. After that parallel data stream is given to IFFT block for the generation of FBMC-FMT signal. Size of IFFT block is (2K-1)N. Where N is number of sub-channels. Then this IFFT output is converted from parallel to serial to get the FBMC-FMT signal. After the generation of FBMC signal it is processed to reduce PAPR of the signal. Here clipping based PAPR reduction technique is used for PAPR reduction of FBMC signal. For this FBMC signal is feed to peak cancellation signal generator block for generating peak cancellation signal. This peak cancellation signal is then subtracted from FBMC signal to clip the portion above clipping level and also this peak cancellation signal is modulated so that it can be added to the clipped FBMC signal without any interference. Then this modulated peak cancellation signal is added with the clipped FBMC signal and converted from digital to analog by using digital to analog converter for transmission through channel.

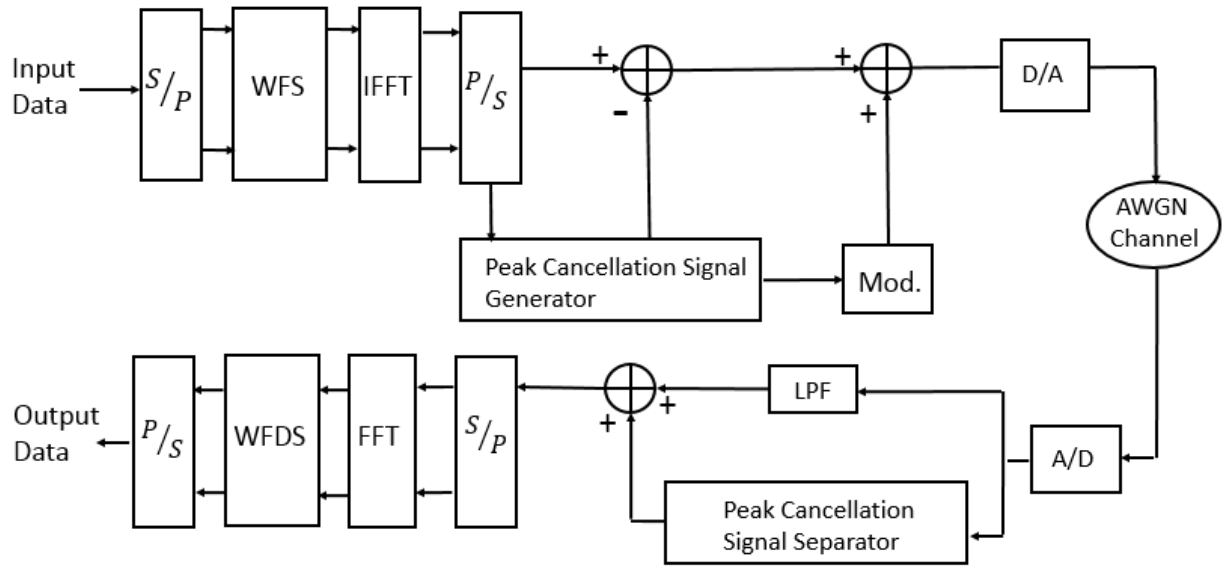

Fig. 4.19 Block Diagram of FBMC-FMT System with proposed scheme

4.3.3.2 Receiver

In the receiver section, signal from transmitter is received through AWGN channel. This received signal is first converted from analog to digital by using A/D converter so that it can

be given to digital processor for demodulation of signal. After analog to digital conversion signal is given to low pass filter and peak cancellation signal separator blocks to separate the clipped FBMC signal and peak cancellation signal. In the LPF block a low pass filter with a cut off frequency equal to the frequency of highest sub-channel is use. In the peak cancellation signal separator block after demodulation, we get peak cancellation signal and add this with filtered clipped signal to get back the original FBMC signal. Then this FBMC signal is converted from serial to parallel and then pass through FFT block for demodulation of FBMC signal. Then this signal is pass through weighted frequency dispreading block, where spreaded data is filtered and added up to get the original data element. After this data elements are converted from parallel to serial to get back the original input data stream.

4.3.3.3 Results and Discussion

Simulation is performed for FBMC-SMT system with 4-QAM and 16-QAM modulated input signals. Number of sub-channels are N=64 and clipping level A is taken as 5 dB above the average power level. Fig. 4.20 show the CCDF plot for original FBMC-FMT, clipped signal and combined signal for 4-QAM modulated signal. Plot shows that PAPR performance improves significantly by clipping technique and combining clipped signal with peak cancellation signal reduces PAPR value by only small amount. Which can be tolerate as this signal gives higher BER performance compared to clipped signal. Fig. 4.21 show the CCDF plot for original FBMC-FMT, clipped signal and combined signal for 16-QAM modulated signal. Comparing these plots we can say that there is some improvement in performance for 16-QAM compared to 4-QAM.

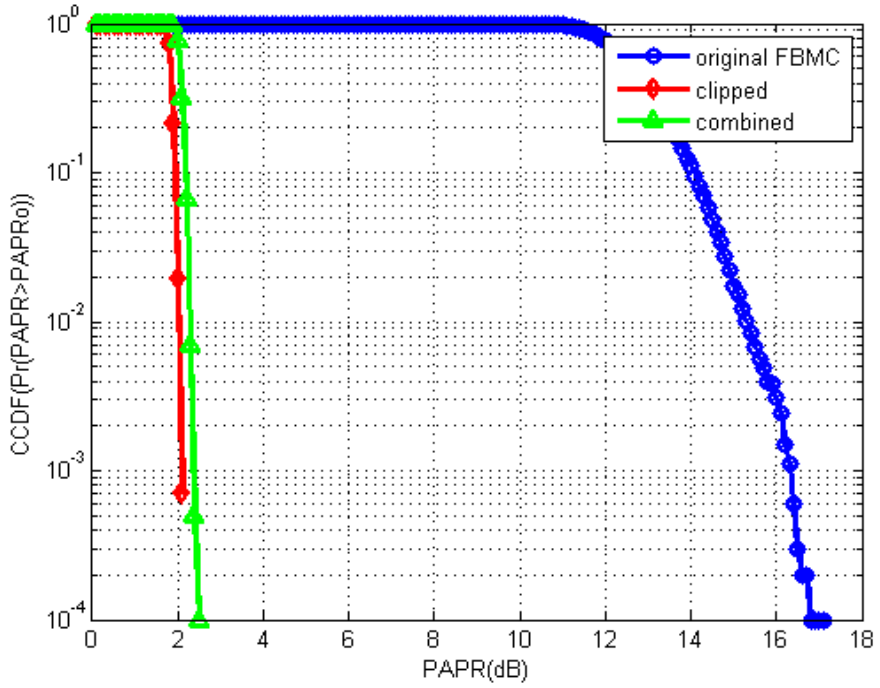

Fig. 4.20 CCDF Plot for original FBMC-FMT signal, clipped signal and combined signal (4-QAM).

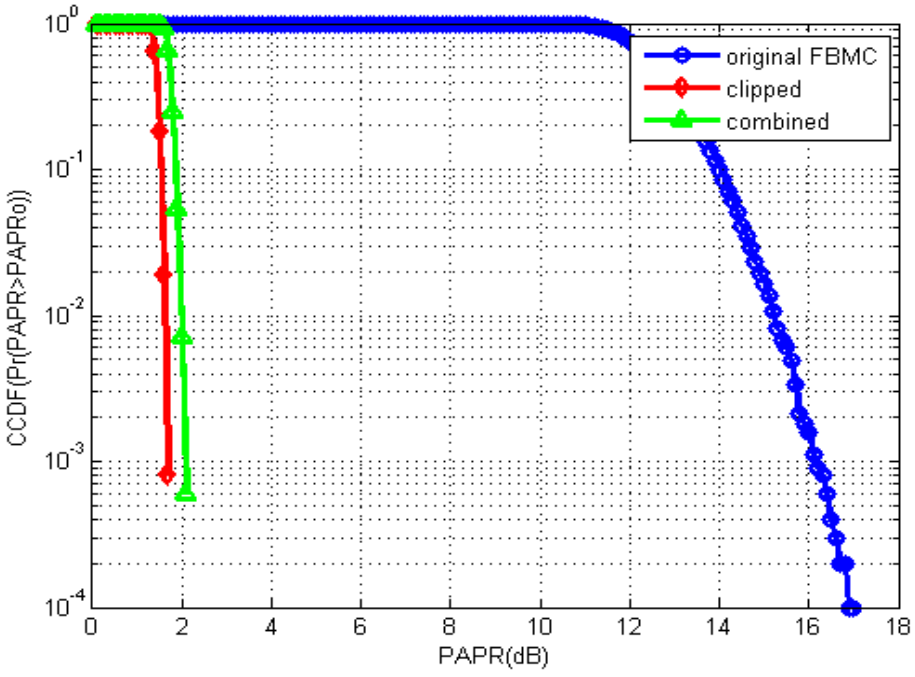

Fig. 4.21 CCDF Plot for original FBMC-FMT signal, clipped signal and combined signal (16- QAM).

4.3.3.4 Power Amplifier (PA) Efficiency Calculation

Table 4.5 contains PAPR values for different PAPR reduction technique and original FBMC signal for 10^{-3} clip probability and efficiency of PA for different PAPR reduction techniques.

Table 4.5 PAPR and efficiency comparison for FBMC-FMT system with new clipping based PAPR reduction technique.

	PAPR(dB) (4-QAM)	η (4-QAM)	PAPR(dB) (16-QAM)	η (16-QAM)
Original FBMC-FMT signal	16.4	1.15	16.1	1.23
Clipped signal	2	31.54	1.7	33.80
Clipped with peak cancellation signal	2.3	29.44	2	31.54

Chapter 5

CONCLUSION

5
CONCLUSION

5.1 Conclusion

FBMC is a promising waveform candidate for 5G technology which gives high spectral efficiency and low out of band radiation required for 5G communication. There are several PAPR reduction techniques proposed for mcm system. Tone injection and companding are two techniques for PAPR techniques. Here a combined scheme of these two techniques is proposed which gives significant PAPR performance improvement compared to those two techniques. Simulation is performed and results are plotted in the form of CCDF plot. Results shows that PAPR performance improves as we combine tone injection and companding techniques. FBMC is generated by using FMT and SMT methods, also 4-QAM and 16-QAM modulated input signals are used for simulation. Comparing the simulation results we can conclude that PAPR performance is almost same for FMT and SMT methods and there is a significant performance improvement as we increase the constellation size with normalization.

Receiver section is also designed to test the transmitted signal over the channel .AWGN channel is used for modelling and simulation of transmitter and receiver section. Simulation is performed to get SER plot. Results shows that symbol error performance of combined scheme is better than companding technique but some degradation in performance compared to original FBMC signal.

Clipping technique has a promising PAPR reduction capability but its SER performance is poor. Here a new clipping based PAPR reduction scheme is proposed, in which we transmit clipped off portion with clipped FBMC signal. So in this way we can improve PAPR performance without degrading SER performance. Simulation is performed for this technique with all three FBMC generation methods (CMT, SMT and FMT). Here also PAPR performance of FMT and SMT are almost similar but performance of CMT is less than other two methods. Also a significant performance improvement is observed as we increase the constellation size with normalization.

5.2 Limitation of the work

In this thesis main focus is towards PAPR reduction of FBMC system with less intension to complexity issue. Also for transceiver design only AWGN channel is considered with baseband modelling.

5.3 Future work

- Hardware implementation of combined scheme of tone injection and compading techniques.
- Design of receiver section for new clipping based PAPR reduction techniques and evaluation of SER performance.

DISSEMINATION:

Gopal, R.; Patra S.K. "**Combining Tone Injection and Companding Techniques for PAPR Reduction of FBMC-OQAM System**" *IEEE Global Conference on Communication Technologies (GCCT 2015),* Noorul Islam University, Kanyakumari, Tamilnadu, India, pp, 709-713, Apr 2015

BIBLIOGRAPHY

[1] Cheng-Xiang Wang; Haider, F.; Xiqi Gao; Xiao-Hu You; Yang Yang; Dongfeng Yuan; Aggoune, H.; Haas, H.; Fletcher, S.; Hepsaydir, E., "Cellular architecture and key technologies for 5G wireless communication networks," *Communications Magazine, IEEE* , vol.52, no.2, pp.122,130, February 2014

[2] M. Schellmann, Z. Zhao, H. Lin, P. Siohan, N. Rajatheva, V. Luecken, and A. Ishaque, "Fbmc-based air interface for 5g mobile: Challenges and proposed solutions," in Cognitive *Radio Oriented Wireless Networks and Communications (CROWNCOM)*, 2014 9th International Conference on. IEEE, 2014, pp. 102–107.

[3] M. Bellanger, D. Le Ruyet, D. Roviras, M. Terr´e, J. Nossek, L. Baltar, Q. Bai, D. Waldhauser, M. Renfors, T. Ihalainen et al., "Fbmc physical layer: a primer," PHYDYAS, January, 2010.

[4] FP7 PHYDYAS Project-D5-1.http://www.ict-phydyas.org/delivrables/PHYDYAS-D5-1.pdf

[5] B. Farhang-Boroujeny "OFDM versus filter bank multicarrier", *IEEE Signal Process*. Mag., vol. 28, no. 3, pp.92 -112 2011

[6] A. Sahin, I. Guvenc, and H. Arslan, "A survey on multicarrier communications: Prototype filters, lattice structures, and implementation aspects," *Communications Surveys & Tutorials*, IEEE, vol. 16, no. 3, pp. 1312–1338, 2014.

[7]Seung Hee Han; Jae Hong Lee, "An overview of peak-to-average power ratio reduction techniques for multicarrier transmission," *Wireless Communications, IEEE* , vol.12, no.2, pp.56,65, April 2005

[8] R.W. Bauml, R.F.H. Fischer, and J.B. Huber." Reducing the peak-to-average power ratio of multicarrier modulation by selected mapping*." Electronics Letters*, 32(22):2056 – 7, 1996/10/24.

[9] Xiaodong Li and Jr. Cimini, L.J. Effects of clipping and filtering on the performance of ofdm. *IEEE Communications Letters*, 2(5):131 – 3, 1998/05/.

[10] A.E. Jones, T.A. Wilkinson, and S.K. Barton." Block coding scheme for reduction of peak to mean envelope power ratio of multicarrier transmission schemes*." Electronics Letters*, 30(25):2098– 9, 1994/12/08.

[11] S. H. Mller and J. B. Huber." Ofdm with reduced peaktoaverage power ratio by optimum combination of partial transmit sequences." Elect. Lett., 33(5):36869, Feb 1997.

[12] B.S. Krongold and D.L. Jones." PAPR reduction in OFDM via active constellation extension." Volume vol.4, pages 525 – 8, 2003

[13] T. Jiang, Y. Yang, and Y. Song, "Exponential companding transform for PAPR reduction in OFDM systems", *IEEE Trans. Broadcasting*, vol. 51,no. 2, pp. 244248, Jun. 2005.

[14] T. Wattanasuwakull and W. Benjapolakul, “Papr reduction for ofdm transmission by using a method of tone reservation and tone injection,” *in Information, Communications and Signal Processing*, 2005 Fifth International Conference on. IEEE, 2005, pp. 273–277.

[15]Tuna C.,Jones D.L.,“Tone Injection with Aggressive Clipping Projection for OFDM PAPR Reduction”*Acoustic Speech and Signal Processing*(ICASSP),2010 IEEE International Conference, pages: 3278-3281

[16]Mishmy T.S.,Sheeba V.S.,“Hybrid companding and coding for Peak to Average Power Ratio reduction in Filter Bank based Multicarrier System”*control communication and computing* (ICCC),2013 International Conference, pages :506-510

[17]N. van der Neut, B. Maharaj, F. de Lange, G. Gonzalez, F. Gregorio, and J. Cousseau, “Papr reduction in fbmc systems using a smart gradient project active constellation extension method,” *in Telecommunications* (ICT), 2014 21st International Conference on. IEEE, 2014, pp. 134–139.

[18]Kollar, Zs.; Varga, L.; Czimer, K., "Clipping-Based Iterative PAPR-Reduction Techniques for FBMC," OFDM 2012, 17th International OFDM Workshop 2012 (InOWo'12); Proceedings of , vol., no., pp.1,7, 29-30 Aug. 2012

[19] Deepa, T.; Kumar, R., "Performance analysis of μ-law companding & SQRT techniques for M-QAM OFDM systems," *Emerging Trends in Computing, Communication and Nanotechnology* (ICE-CCN), 2013 International Conference on , vol., no., pp.303,307, 25-26 March 2013